| | |
|---|---|
| AP42 Section: | 7.1 |
| Related | 2 |
| Title: | Internal Floating Roof Technical Analysis<br><br>Robert McAllister, TRW, Inc.<br><br>January 1983 |

A-80-51
II-A-21

# INTERNAL FLOATING ROOF TECHNICAL ANALYSIS

by

Robert A. McAllister, Ph.D., P.E.

TRW Incorporated
Energy and Environmental Division
Research Triangle Park, North Carolina 27709

January 1983

for

Chemicals and Petroleum Branch
Office of Air Quality Planning and Standards
United States Environmental Protection Agency
Research Triangle Park, North Carolina 27711

## INTRODUCTION

A theoretical analysis of the emission mechanisms occurring from internal floating roof tanks was conducted. It was quickly apparent that the roof configurations and the fluid flows were more complex than would permit a complete model to be derived from theoretical considerations alone. Nevertheless, to aid in the basic understanding of the emission mechanisms and rates, a theoretical analysis was done as rigorously as possible in a short length of time. The theory was useful in examining (primarily) the Chicago Bridge and Iron Company data (March 1982) on internal floating roof emissions for internal consistency and for drawing appropriate conclusions.

It is to be noted that the conclusions that may be drawn pertain primarily to the CBI report and not to the overall American Petroleum Institute study.

# INTERNAL FLOATING ROOF TECHNICAL ANALYSIS

A. Why does an internal floating roof tank reduce emissions, compared to a fixed-roof tank? Describe the primary loss mechanisms in internal floating roof tanks.

The free surface of liquid is greatly reduced in an internal floating roof, compared to a fixed-roof tank. The implication here is that equilibrium does not occur. Therefore, the evaporation is proportional to the free surface of liquid.

Primary Loss Mechanisms, Internal Floating Roof Tank

1. Standing storage losses
    a. Rim seal loss
    b. Deck seam loss
    c. Deck fitting loss
    d. Other losses.

The relative amounts of the above can be calculated from the API formulas appearing in the API Draft 2519 Bulletins.

The rim seal loss equation used in API Draft 2519 Bulletin uses essentially the same form as in API 2517 for External Floating Roof with the exception that for internal floating roof losses, there is no air velocity term in the equation. API states that (API 2519, p. 34) a statistical analysis of all emissions vs. wind-speed data demonstrated that the emission estimates are not improved by including windspeed in the analysis. The API statistical analysis was not evaluated in this study. The flow between the vapor mounted rim seal and the tank wall is assumed to be laminar, although there are no data to support the assumption of laminar flow.

As wind blows across the top of the internal floating roof, the static pressure on the top of the rim seal is reduced on the windward side* and is increased on the leeward side ($180^{o}$ from the direction of approach of the wind to the tank). The API model for rim seal losses has air entering the vapor space between the vapor-mounted seal and the exposed liquid surface. The air enters between the rim seal and the interior tank wall, and is assumed to be in laminar flow. In the theoretical model considered to describe this flow (see Equation 1 and 8, and Figure 1), it was assumed that the cross-section flow area was a thin slit (seal gap) of height, "b", and width equal to the seal perimeter, $\pi D$ (where D is the tank diameter). Thus the flow would be past parallel plates a distance of "b" apart and width $\pi D$. The length of path of the flow between the rim seal and the tank was not postulated, but would be surely less than 10 cm. The API model also had the air entering the rim seal on the windward side flowing around the perimeter of the tank and out the rim seal on the leeward side. The flow between the rim seal and the tank on the leeward side was also assumed to be laminar. The flow in the vapor space under the rim seal around the circumference was assumed to encounter less resistance than the flow between the rim seal and the tank. While traveling around the perimeter of the tank in the rim seal vapor space, the air was assumed to be saturated with vapors of the liquid being stored.

For the rim seal losses, the temperature effects are imbedded in the pressure function P* and in $K_R$ in Equation 12 of the Appendix. The vapor pressure, p, increases exponentially with temperature. A common equation relating p with temperature is the Antoine equation $\ln p = A - B/(t+C)$. For normal hexane A=6.9130, B=1187.8, C=225.947, $t=^{o}C$, p=mmHg. In the original derivation of the rim seal loss equation, K should be a function of temperature, since K, see Equation 11 contains $\rho^2$ in it and $\rho$ is a function of temperature.

---

*Note that the "windward" side depends on the point of view. If one looks at a storage tank, the "windward" side is the side that the wind strikes first. That is the perspective spoken of here. If there is a wind blowing from the North to the South, the windward side would be the North side of the tank. The "leeward" side is the South side. On the other hand, if one looks at the wind flow from the point of view of an observer inside the tank on the roof, then the "windward" side would be the South side of the tank since that is the first side the wind strikes. The north side of the roof or rim seal would be the leeward side.

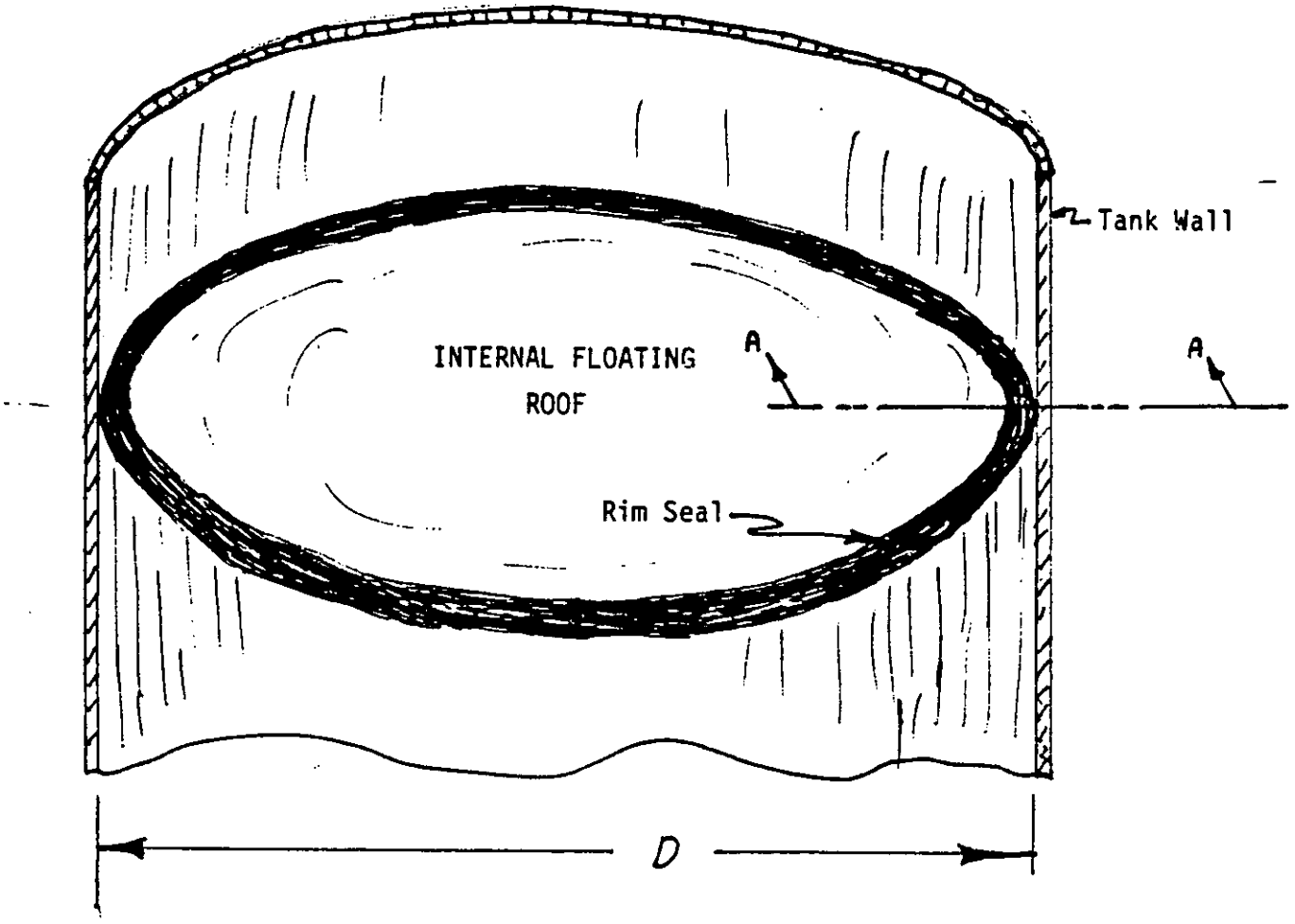


SECTION A-A

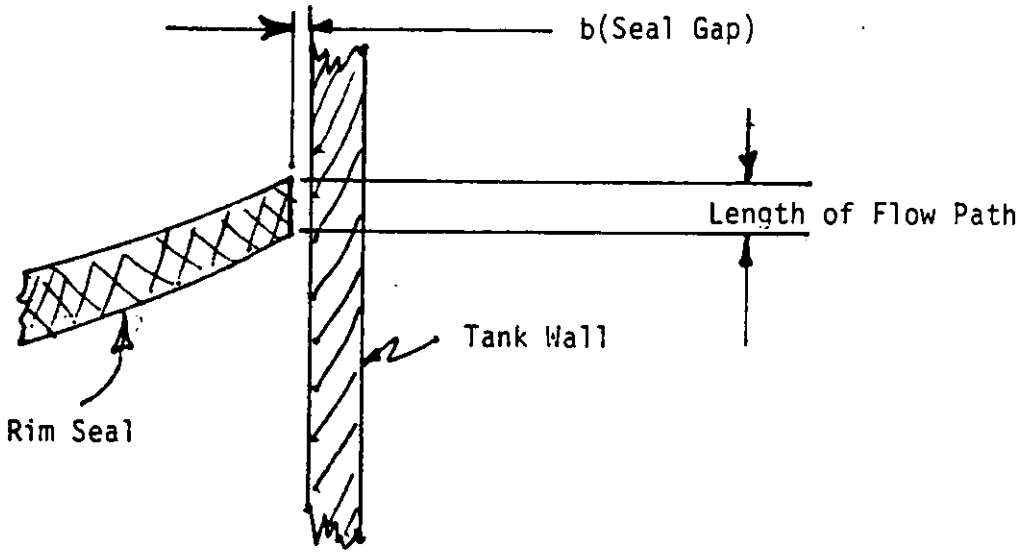


Direction of flow is verticle between rim seal and wall.

Figure 1. Flow path for rim seal losses.

$$\rho_A = \frac{p\ M_A}{RT}$$

$$\rho_A^2 = \frac{(pM_A/R)^2}{T^2}$$

The API correlation (API 2517 or 2519) does not recognize K in Equation 8 or 11 as a function of temperature. On the other hand, the tests used in the rim seal analysis range in temperature from $50^oF$ through about $85^oF$. Part of the temperature variation is accounted for in the API P* function. The K in the API formula may then be viewed as an average K over the temperature range.

It is not clear whether K should be inversely proportional to the temperature squared, because Equation 11 is based on the laminar flow equation, and in my opinion laminar flow past the rim seal has not been established. If the flow through the rim seal is turbulent, the pressure function, and temperature dependence of K would be different, as can be seen by comparing Equations 1 and 6. One could point out flow in an internal floating roof should be more nearly laminar than for the external floating roof, in which the $(P_L - P_W)$ terms are larger. The function P* in Equations 9, 10, and 12 was derived starting with Equation 1, which assumes laminar flow. If turbulent flow is assumed, or if another form of the laminar flow equation (similar to Equation 3) is used as the starting point, the pressure function P* no longer takes the form given in Equation 10. In a brief analysis done by TRW the function $(P/14.7)^{0.7}$ seemed to give a better scaling factor for the vapor pressure than P*. The API rim-seal loss formula, Equation 12, assumes the emission loss through the seal to be independent of velocity. Visual examination of the data in the CBI Report does not confirm this assumption. In some cases the slopes of the curves of evaporation losses vs. wind velocity, on a log-log plot, are not statistically different from zero (Figure 3-5 and 3.4) but in other cases, the slopes are clearly greater than zero (e.g. Figure 2-13, 2-17, and 3-3 of the CBI Report of March 1982). A statistical analysis could be done to determine which seal configurations give slopes statistically different from zero. A zero velocity effect, or a zero slope would imply a term, $V^{0.0}$, in evaporation loss Equation 12.

An additional rim seal loss not accounted for in the API formulas is the permeation through the rim seals. This is probably a negligible amount compared to the rim seal loss due to hydrodynamic forces for vapor mounted seals. There may be sufficient data in the CBI study to investigate this effect further (see recommendation no. 4).

Some authors claim that permeation of a liquid through a polymeric material can be 1000 times as rapid as permeation of a vapor. More recent careful studies have shown, however, that permeation of a liquid is the same as permeation of a saturated vapor, as would be expected from thermodynamic principles. If the liquid "wets" the liquid mounted seal, it could pull liquid up between the wall and the seal by capillary action, even though the seal is 6 inches thick or more. The API tests did not observe such an occurrence and it was not considered important. The API test data suggest that liquid mounted seals permit less emissions than the vapor mounted seals.

Deck fitting losses are essentially controlled by Equation 18. It is not possible to calculate k a priori, but k is a function of the configuration of the opening, the velocity of the wind blowing across it, and the Schmidt number of the diffusing material (see Equation 19). It would have been better if CBI had conducted the evaporation-loss experiment with air blowing across the top of the fitting. See groupings in Table C-1 in Appendix C. The deck fitting loss is probably proportional to the velocity to some exponent. The data shown in the Appendix C (see reprint) gives a velocity exponent of 0.8, but for deck fittings I would expect it to be greater than 1.0. The effect of turbulence on the liquid surface in the case of the deck fittings should be greater than for the reprint, therefore, the exponent on the velocity term should be greater than 0.8. It is expected that all the deck fitting emission losses in the API report are underestimated.

Table C-1 in Appendix C analyzes the CBI data on emissions from IFR Deck Fittings. As indicated in Equation 19 of the Appendix, a number of

correlations have been done on various kinds of mass transfer configuration and based on dimensional analysis which suggests that

$$\frac{kD\overline{M}}{\rho D_v} = a\left(\frac{Du\rho}{\mu}\right)^b \left(\frac{\mu}{\rho D_v}\right)^c \qquad (19A)$$

The exponents in Equation 19A are independent of the vapor that is undergoing diffusion or the medium through which diffusion is occurring. The exponents are a function of the physical configuration, i.e. the shape and flow patterns of the liquid surface and the flow patterns of the vapor in contact with the liquid. Thus Equation 19A applied to free evaporation from a liquid spill becomes

$$kg = \frac{0.0292\ do^{-0.11}}{RT}\ u^{0.78}\ Sc^{-0.87} \qquad (19B)$$

as shown in the reprint in the Appendix. Note that $Sc = (\mu/\rho D_v)$.

In Table C-1 of the Appendix C, $(WA/A)_A$ is the actual gm/($cm^2$day) measured for the indicated CBI test run. (WA/A) for a mass rate of mass transfer corresponds to (NA/A) in Equation 18 for a mole rate of mass transfer, since $(y_{Ai}-y_A)$ in Equation 18 is approximately the same for all the CBI runs, $(WA/A)_A$ is proportional to k for each test and configuration of deck fitting (described in the final column of Table 2). $(W_A/A)_D$ is the calculated value of the mass transfer rate if only diffusion of hexane is involved. Therefore, the ratio $(WA/A)_A/(WA/A)_D$ is a proportional measure of the role of convection in the mass transfer, i.e. the higher the ratio, the greater is the role of convection. The factor k includes both the mass-transfer effects of diffusion combined with the effects of convection.

For the 1/8" gap note that the ratio $(WA/A)_A/(WA/A)_D$ is the largest for the double channel column openings, Tests 12 and 15. This result should be expected since the complex double channel column would cause lots of eddy currents simply because of the geometrical complexity of the fitting for the 1/8" gaps in which there was simply a circular pipe or circular drum involved, Cases 5 and 13, the value of the ratio $(WA/A)_A/(WA/A)_D$ is much less and about 5.

Tests involving a 1/2" gap, Runs 3 and 8, show about the same value of the ratio although a circular pipe is involved in one case and double channels in the other. At zero velocity across the top of the drum, at least the two values are the same order of magnitude, although this may not be the case at higher velocities, since the convective contribution to mass transfer (evaporation of the liquid) should be higher for the double channel case.

Test 4 looks inordinately low because none of these ratios should be less than 1.0. Furthermore, since it was an unshielded 8" hole (with slotted sample well), one would expect a great deal of natural convection, and much more than, for example Runs 5 and 13 or for Run 6 with the 1" hole.

For tests 6 and 14 there were well protected holes with little opportunity for natural convection and the ratio $(WA/A)_A/(WA/A)_D$ are about equal at 2.25.

For each set of tests which gave approximately the same values of $(WA/A)_A/(WA/A)_D$ which had the same of similar fitting configuration, one should be able to derive an equation similar to Equation 19A or 19B. This would require measuring the evaporation rates at various values of velocity.

Deck seam losses have been shown in the recent CBI/API study to be a significant contributor to emission losses. If one assumes that the cracks or openings are small enough to prevent liquid flow, then the mechanism for mass transfer must be by diffusion rather than by bulk flow of the fluid, primarily. As seen by Equation 13, the rate of diffusion is inversely proportional to the length of the diffusion path. Thus diffusion through a 2-inch thick panel seam should be one-half that through a one-inch thick panel seam. For a bolted non-contact deck seam, the width of the overlap would determine the length of the diffusion path. For a contact roof that wets the liquid the deck seams could act as capillaries to draw liquid into the seam, thus shortening the length of the diffusional path. Equation 13 shows the rate of diffusion to be proportional to the cross-sectional area, the diffusivity coefficient, the vapor molar-density and $\ln((1-y_A)/1-y_{Ai}))$. The cross-sectional area

for diffusion should be directly proportional to the length of deck seams. Molar density is directly proportional to atmospheric pressure and inversely proportional to temperature. The diffusion coefficient is proportional to the 1.81 power of the temperature as shown by Equation 14. The temperature dependence of the diffusivity coefficient is not clear in Equations 15 and 16 because of the temperature dependence of the collision integrals, which is generally given in tabular form. The logarithm term in Equation 13 is temperature dependent through $y_{Ai}$ which is approximately $p_{Ai}/\pi$, where $p_{Ai}$ is the vapor pressure of the diffusing component, and $\pi$ is the total pressure. As the temperature increases, the $\ln((1-y_A)/(1-y_{Ai}))$ term increases because of the increase of the $y_{Ai}$ term.

At least two other phenomena are at work in an internal floating roof tank which are not taken into account in the API formulas. It is not easily possible to evaluate either of these theoretically. The first phenomenon is the effect of diurnal temperature changes on the rate of emissions. The second is the effect of mechanical flexing of the internal floating roof on the emission rate.

In examining diffusional breathing losses, the following analysis can be made. If the temperature cycled as a saw-tooth wave, during the day increasing $10^{o}C$, and decreasing $10^{o}C$ at night from an average T for the 24-hour daily period, the overall emissions for diffusional breathing losses should be higher than if the temperature remained constant at T all day long. Table 1 shows the calculation for the temperature dependence of the diffusional mode of emission. For this mode a 68 percent increase in the flux would occur if the temperature were raised from $20^{o}C$ to $30^{o}C$. If the temperature dropped to $10^{o}C$, only a 41 percent decrease in the diffusional rate would occur for benzene diffusing through air at one atmosphere total pressure. For mass transfer involving convection (Equation 18), a similar result would be expected, although no theoretical expresssion can be derived at this time. It is to be noted that convection is a combination of molecular diffusion and turbulent, eddy flow. It would be expected that for convective flow the mass transfer rate increase for a $10^{o}$ temperature rise would be greater than the mass transfer rate decrease for a $10^{o}$ temperature drop.

Table 1. CALCULATION OF DIFFUSIONAL EMISSION FLUX FOR BENZENE

| t, $^{o}C$ | $p^{o}$, mm | $y_{Ai}$ | $\ln \frac{1}{1-y_{Ai}}$ | $\rho_t$ | $(D_v)_t$ | $\frac{(N_A/A)_t}{(N_A/A)_{20}}$ | Decrease/ increase from 20°C |
|---|---|---|---|---|---|---|---|
| 10 | 45.19 | 0.0595 | 0.0613 | $1.035\rho_{20}$ | $0.939\ (D_v)_{20}$ | 0.581 | 41% decrease |
| 20 | 74.13 | 0.0975 | 0.1026 | $\rho_{20}$ | $(D_v)_{20}$ | 1.000 | |
| 30 | 117.45 | 0.1545 | 0.1678 | $0.967\rho_{20}$ | $1.0624(D_v)_{20}$ | 1.680 | 68% increase |

@20°C

$$\frac{N_A}{A} B_T = D_v \rho \ln \frac{(1-y_A)}{(1-y_{Ai})} = 0.1026\ (D_v)_{20}\ \rho_{20}$$

@10°C

$$\frac{N_A}{A} B_T = (0.0613)(1.035)(0.939)(D_v)_{20}\rho_{20} = 0.0596\ (D_v)_{20}\rho_{20}$$

@30°C

$$\frac{N_A}{A} B_T = (0.1678)(0.967)(1.0624)(D_v)_{20}\rho_{20} = 0.1724\ (D_v)_{20}\rho_{20}$$

Roof flexing could become a significant factor, especially for roofs greater than 100 feet. The roof can be visualized as a large "membrane" similar to a drum head. A vapor mounted roof would be more susceptible to vertical flexing than a liquid mounted roof, since the latter would be damped by the liquid surface on which it rests. In actual practice there are local pressure and velocity gradients due to changes in wind velocity and wind turbulence across the roof surface. In the absence of a roof one can see the effect of local wind velocity and pressure fluctuations on the surface of a lake. For a local pressure increase of 0.1 $lb/in^2$ acting on 1/100 of the surface of a 100-feet roof, the effect is 1,130 pound force, which would locally flex the roof, setting up a vertical vibration which would dampen. The case given is, of course, exaggerated, in terms of the magnitude of the possible forces, but with any span larger than 25 feet vibrations probably are measurable. Such movement would increase turbulence around deck fittings and the rim seal and deck seals and increase overall emission rates. For a liquid mounted roof such flexure would not be as significant as for a vapor mounted roof. But even on a liquid surface there is probably measureable flexing for 100-foot roofs and larger. API has not considered the possibility that such an effect might be significant. In any case, the API data have measured overall emissions, but not attempted to separate out a component due to flexing.

B. Can some roof types reduce emissions significantly more than others?

It is fairly clear that some types of roofs can reduce emissions more than others. A welded roof for example can reduce emissions compared to a bolted roof, other design specifications being the same, because of the elimination of the deck seam losses. Roofs with secondary rim seals generally reduce emissions compared to roofs with primary seals only. Not only do the secondary rim seals reduce the probability of a gap at any angle $\theta$ around the top of the IFR, but the secondary rim seal also reduces the $\Delta P$ (the hydrodynamic driving force for flow) between the primary rim seal and the vapor space in contact with the liquid. The rim seal loss should be greatly reduced.

Liquid-mounted rim seals reduce emission losses compared to vapor mounted rim seals because of the reduced free surface area of liquid and because of the elimination of gas flow in the rim vapor space. Emission losses for liquid-mounted rim seals are expected to derive from any gaps between the seal and the wall, from permeation of the liquid through the seal, and from evaporation from free liquid surfaces resulting from capillary action which draws liquid up in small openings between the seal and the wall.

B.1 Are losses affected by a vapor space under the roof and rim seal? If so, how does the size of the vapor space under the roof affect losses from deck fittings and deck seams and how does the size of the vapor space under the rim seal affect losses from that seal?

My judgement is that a vapor space under the roof affects the overall losses. With the same design for deck fittings, the deck-fitting losses should be the same for contact and non-contact roofs, with one possible exception. First of all for a non-contact roof, the flexural deformation for the internal floating roof should be greater than for a contact roof. This would give more turbulence around deck fittings and associated free liquid surfaces, resulting in increased emission losses, as discussed above.

Insofar as deck seam losses per foot of seam are concerned, the liquid mounted seam would be expected to emit at a higher rate compared to the vapor mounted deck seam of the same design. Consider for example a bolted deck of metal sheets. Presumably the seams are bolted sufficiently tight so that bulk flow of liquid or vapor is essentially zero. The assumption here is that if the crevices in the seams are large enough to have significant flow through them due to a pressure difference (say for a non-contact floating roof), then the crevice would cause serious flow (or wicking) in the case of the contact floating roof. Therefore, all the emissions are assumed to be diffusional in this comparison. For diffusional emissions there is no difference in total pressure across the seam. The entire emission loss from the deck seam can be attributed to molecular diffusion since there is a partial pressure difference

across the seam, and thus a concentration difference. Equation 13 shows the driving forces and molecular flux resulting from diffusion. For the contact roof floating in a wetting liquid, the liquid would be drawn into the seam by capillary action thus significantly reducing the length of the diffusional path. Equation 13 shows the rate of diffusion to be inversely proportional to the diffusional path so one would expect the diffusional losses per foot of seam from contact internal floating roofs to be greater per foot than for non-contact roofs, assuming that the seam dimensions are the same for both.

The size of the vapor space under the roof should not affect any loss mechanism discussed above so long as there is a vapor space. If the roof is intermittently in contact with liquid and vapor, some of the effects discussed would be blurred.

The dynamic effect of temperature changes throughout the day and their affect on emissions has been discussed briefly above. Considering the effect of temperature changes above a contact vs. a non-contact roof and their effect on emissions would primarly be a function of the rates of heat transfer. One would expect the temperature changes to affect a contact roof more significantly than a non-contact roof, since the heat-transfer coefficient between a solid and liquid surface is greater than between a solid and vapor surface. Thus the liquid surface in the contact roof would heat faster than the liquid surface in a non-contact roof. Any mechanism that uses partial pressure (or concentration, or mole fraction) as the driving force would increase the emission rate due to increase in the liquid surface temperature. Thus both deck-seam losses and deck fitting losses, and rim-seal losses should be larger for contact roofs compared to non-contact roofs.

The volume of the rim-seal space should not be a factor in affecting the rim seal losses, except that the assumption is made in the original derivation that the resistance to flow around the circumference of the rim seal is less than the resistance to flow vertically past the rim seal. So long as there is about 5 cm. or more between the liquid surface and the bottom of the rim seal the assumption should be valid, and the emissions past the rim seal should be independent of the volume of the rim seal space.

B.2 Can losses due to seal and gasket permeation by benzene (and other chemicals) be significant?

The answer to the question is probably not, assuming that benzene (or other chemical) does not deteriorate the gasket. The data in the CBI report suggest that benzene permeates neoprene and other gasketing material 10 times (or more) faster than hexane or other hydrocarbons. The data in the CBI report are conflicting on that point. Data from the literature show a wide range of permeabilities of benzene compared with hydrocarbons such as hexane. In some cases the magnitudes are comparable, but in several cases the permeability of benzene is much higher by a factor of 10 or even 100. This effect seems to depend on the polymeric material and whether the benzene solubility coefficient is high. The synthetic rubbers seem to have a higher permeability for benzene than for hexane. There are no theoretical bases for predicting permeation rates through polymers.

In the CBI testing it is not clear whether breakthrough time was ever accounted for in determining "average" permeation rates. When the permeating fluid, liquid or vapor, is first brought in contact (zero time) with a membrane through which permeation takes place there is a period of time before any of the permeate appears downstream of the membrane. The time between zero time and the time of finding permeate on the downstream side of the membrane is called the breakthrough time. During the breakthrough period, the permeating material is interacting with the membrane in something like a solvation or sorption mechanism. Ignoring the breakthrough time in the data analysis could significantly affect the "average" permeation rate. It is clear that the CBI method of calculating the permeation rates is incorrect, see analysis below on Permeation rates. The CBI report used a gross average permeation rate instead of a differential rate.

C. Is it possible to estimate the contribution of fittings, seams, and seal losses? If so, does the test data support this?

It is not possible theoretically to predict the contribution of fittings, seam, and seal losses. Given sufficient data, however, it would be possible to correlate the parameters so that in the future, the losses could be predicted with confidence. See the analyses given below.

For the fitting losses, one needs to have values for k in Equation 18 which currently can only be determined from actual data. Furthermore a relation such as Equation 19 needs to be developed to determine the velocity dependence and the characteristic dimensions and fluid-property dependences which affect k.

For the seal losses a better characterization of the flow, and even the mechanism of the loss needs to be postulated and verified. The fact that the seal does not fit as tightly around the circumference is a problem in characterizing the flow. Furthermore, the length of the flow path past the rim seal is not characterized very well. The friction factors involved with this type of flow are virtually indeterminant and friction factors even in smooth tubing and round pipe have eluded theoretical analysis. They are all currently empirical.

The analysis which follows shows some analysis of the test data. Time did not permit a critical theoretical analysis of the test data separating out the various component losses.

## CONCLUSIONS AND RECOMMENDATIONS

1. It is not clear whether the API 2519 is assuming laminar flow past the seal for rim seal losses. In any case, laminar flow is not established experimentally as the mechanism in the CBI data.
2. The rim seal loss factor, $K_R$, should be a function of temperature.
3. The assumption of the velocity independence of the rim seal losses is not supported by the data. A statistical analysis is recommended to determine the velocity dependence.
4. Permeation of vapor or liquid through the rim seals may be a significant factor. This mechanism should be investigated further.
5. Estimations show that for seals (liquid or vapor) using materials that are not adversely affected by the stored liquid, and that are of an appropriate thickness, the contribution of permeation through the seals is probably negligible.
6. For liquid mounted seals, capillary action may cause exposed liquid to be present between the seal and the tank wall. This possibility should be investigated further.
7. Deck fitting losses should be a function of the air velocity passing over the fitting. The losses should also be a function of the material being emitted, e.g. propane, octane, benzene, etc. There should also be a product factor for deck fitting losses.
8. Deck seams should emit greater amounts for contact roofs than for non-contact roofs of essentially the same seam design. This proposition should be investigated further.

9. The effect of diurnal temperature changes should result in higher emissions that would be expected by calculating the emissions at an average temperature. It is recommended that this proposition be investigated.

10. The effect of flexure of the internal floating roof on the rate of emissions should be studied further.

11. The CBI data on permeation of hexane through urethane-coated nylon fabric are inconsistent.

12. The CBI data for the diffusion of hexane into air from a Type I apparatus (see Table 5.5) is about 20 percent higher than the theoretical calculation.

13. The CBI data for the diffusion of benzene into air from a Type I apparatus agrees with the theoretically calculated value.

14. Emissions for Test 4 of the CBI data (evaporation losses from an 8-inch diameter slotted sample well) seems inordinately low, by more than a factor of 10.

15. Deck seam losses should be independent of air velocity over the roof, if diffusion controls the losses.

16. The data used to separate the rim seal losses, the deck fitting losses, and the deck seam losses need to be reviewed further for internal consistency.

17. Additional calculations should be done on the CBI data for diffusion and permeation with Type III apparatus, separating the diffusional flow from the permeation flow. These calculations would further test the internal consistency of the results, and impinge on their conclusions.

# APPENDIX

The appendix contains the basic equations which describe the several mechanisms of flow from an internal floating roof tank. It is divided into three main sections, Hydrodynamic Flows, Diffusional Losses, and Permeation.

Hydrodynamic flows refer to mass flow rates caused by pressure differences (not including permeation). The hydrodynamic flow Equations (1) and (6) give the flow rate for laminar and for turbulent flow between parallel plates, respectively. Equations (2) and (7) give the flow rate equations for laminar and turbulent flow in round pipes. Equations 8 through 11 given rim seal loss equations for external floating roof tanks from API 2517, and Equation 12 gives the rim seal loss equation for the draft API Report 2519.

Mass-transfer equations for diffusional losses and diffusional combined with convectional losses are given in Equation 13 through 19. Equation 13 is the basic equation for diffusional of component A through stagnant component B. Equations 14, 15, and 16 present equations used to calculate the diffusion coefficient $D_v$. Calculations for "straight" diffusion for benzene and hexane in a Type I CPI apparatus are given and compared to the data in Table 5.3 of the CBI report. Equations 17, 18, and 19 give the mass-transfer equations for the case where both diffusion and convection are involved. Equation 19 shows the type of relation needed to correlate the mass-transfer coefficient k, as a function of the physical dimensions of the deck fitting and the wind velocity. Table C-1 shows an analysis of the IFR deck fitting tests, and how the CBI test data might be grouped for further analysis.

The final section of the Appendix gives equations for gas or liquid permeation through polymeric materials. There follows also a comparison of literature values of permeation of benzene and hexane with the CBI data.

# APPENDIX A

## MASS-TRANSFER EQUATIONS

### HYDRODYNAMIC FLOWS

Laminar Flow:

1. Between parallel plates: width = a, height = b
   For a tank, a = $\pi D$, the tank perimeter
   D = inside diameter of the tank, ft.

For b<<a, or a/b = $\infty$,

$$w = \frac{b^3 \rho g_c \pi D \, (p_1 - p_2)}{12 \mu L} \qquad (1)$$

w = weight rate of flow, lb/sec

b = gap between seal and tank, assumed small and uniform around perimeter, $ft^3$

$\rho$ = fluid density, $lb/ft^3$

$g_c$ = dimensional constant, 32.174 $lb\text{-}ft/(lb_f sec^2)$

$\pi$ = 3.17159...

D = tank inside diameter, ft.

$p_1, p_2$ = upstream and downstream static pressures, $lb_f/ft^2$, absolute

$\mu$ = absolute viscosity, lb/(ft-sec)

L = length of flow passage

2. Inside a round pipe, inside diameter D

$$w = \frac{\pi D^4 \rho g_c \, (p_1 - p_2)}{128 \mu L} \qquad (2)$$

For ideal gases $\rho = \frac{PM}{RT} \approx \frac{(p_1 + p_2)}{2} \cdot \frac{M}{RT}$ for which pressure drop is less than 10% of $p_2$.

where

M = molecular weight, lb/lb mole

R = dimensional constant, 1545.3 $(ft^3\ lb_f)/(ft^2\ lb\text{-}mole\ {}^oR)$

T = temperature, ${}^oR$

$$w = \frac{\pi D^4 M g_c \, (p_1^2 - p_2^2)}{256 \mu L} \qquad (3)$$

Turbulent Flow

1. Between parallel plates

$$R_H = \frac{\pi Db}{2(\pi D+b)} \quad (4)$$

$R_H$ = Hydraulic radius = (cross sectional areas of stream)/(wetted perimeter), ft

For b<<D

$$R_H = b/2 \quad (5)$$

$$w = \pi \frac{\rho g_c b^3 (p_1-p_2)}{fL} = \pi \frac{g_c b^3 M (p_1^2-P_2^2)}{fLRT} \quad (6)$$

where

f = Fanning friction factor, dimensionless = $\emptyset(N_{Re})$

$N_{Re}$ = Reynolds number = $DV\rho/\mu$, dimensionless

V = average fluid velocity, ft/sec

2. For a round pipe

$$w = \frac{\pi}{8} \frac{g_c D^2 M (p_1^2-p_2^2)}{fLRT} \quad (7)$$

For external floating roof (Laverman Derivation...)(API 2517)

Beginning with Equation (1) for laminar flow, Laverman derived the following:

Evaporation Loss

$$L = K M_v DV^2 \left\{ \frac{P_v/14.7}{\left[1+\left(1-\frac{P_v}{14.7}\right)^{\frac{1}{2}}\right]^2} \right\} \quad (8)$$

or $L = KM_v DV^2 P^* \quad (9)$

where

$$P^* = \frac{P_V/14.7}{\left[1 \pm \left(1 - \frac{P_V}{14.7}\right)^{1/2}\right]^2} \qquad (10)$$

L = evaporation loss through the rim seal, lb/yr

$P_V$ = true vapor pressure at stock storage temperature, psia

$$K = \frac{(8760)(2600)\ b^3 \rho_A^2}{48 \quad L}$$ , rim seal loss factor $(\text{lb-mole sec}^2)/\text{ft}^3$ (11)

For internal floating roof (draft API 2519)

Evaporation Loss

$$L = K_R K_C M_V D\ P^* \qquad (12)$$

where

$K_R$ = rim seal-loss factor, lb-mole/(ft yr)

$K_C$ = product factor, dimensionless

The Laverman derivation assumes laminar flow between the rim seal and the tank wall. This assumption seems to be based more on convenience than on data. If one begins the derivation using turbulent flow instead of laminar flow, it is not possible to get a pressure function like P*. The pressure function is exceedingly more complex.

My opinion is that laminar flow is unlikely as the major contributor to rim seal losses. The flow is probably transient (a function of time) and neither fully-developed laminar flow nor fully-developed turbulent flow. On the other hand, for a steady wind velocity, I would expect that part of the rim seal losses would be laminar and part would be turbulent. Apparently for internal floating roof cases, $(p_L - p_W)$ and thus the wind velocity dependence on the rim seal loss is less. One would expect a larger percent of the rim seal losses to be laminar for internal floating roofs than for external floating roofs. I do not believe the available data are sufficient to decide between laminar flow and turbulent flow; it is not possible, in my opinion, to calculate theoretically what fraction of the flow is laminar and what fraction is turbulent.

DIFFUSIONAL LOSSES

Diffusion of component A through stagnant component B

$$\frac{N_A}{A} = \frac{D_v \rho_m}{B_T} \ln \frac{1-y_a}{1-y_{Ai}} \tag{13}$$

where

$N_A$ = moles A diffusing/sec
$A$ = cross sectional area for diffusion, $cm^2$
$D_v$ = Diffusion coefficient of A into B, $cm^2/sec$
$\rho_m$ = molar density, g mole/$cm^3$
$B_T$ = length of diffusion path, cm
$y_A$ = mole fraction of component A at b = $B_T$
$y_{Ai}$ = mole fraction of component A at b = 0, the liquid-vapor interface

$$D_v = \frac{0.01498\ T^{1.81} \left(\frac{1}{M_A} + \frac{1}{M_B}\right)^{0.5}}{P(T_{cA}T_{cB})^{0.1405} \left(V_{cA}^{0.4} + V_{cB}^{0.4}\right)^2} \tag{14}$$

where

$T$ = absolute temperature, K
$M_A, M_B$ = molecular weight of A and B respectively, g/(g-mole)
$T_{cA}, T_{cB}$ = critical temperature of A and B, K
$V_{cA}, V_{cB}$ = critical volume of A and B, $cm^3$/g-mole
$P$ = total pressure, atm.

$$D_v = \frac{(0.00107-0.000246\ (\frac{1}{M_A}+\frac{1}{M_B})^{0.5})\ T^{3/2}\ (\frac{1}{M_A}+\frac{1}{M_B})^{0.5}}{P\ (\sigma_{AB})^2\ [f(kT/\epsilon_{AB})]} \qquad (15)$$

$P$ = total pressure, atmosphere

$\sigma_{AB}$ = collision diameter for A and B = $(\sigma_A+\sigma_B)/2$, angstroms

$\sigma_A, \sigma_B$ = collision diameter for A and B, respectively, angstroms

$f(kT/\epsilon_{AB})$ = collision integral for diffusion of A into B, $(kT/\epsilon)$ diminsionless

$k$ = Boltzman's constant

$\epsilon_{AB}$ = collision integral for AB collision = $\epsilon_A\epsilon_B$

$\epsilon_A, \epsilon_B$ = collision integral for A and B, respectively.

$$D_v = \frac{0.001858\ T^{3/2}\ (\frac{1}{M_A}+\frac{1}{M_B})^{\frac{1}{2}}}{P\ (\sigma_{AV})^2\ \Omega_D} \qquad (16)$$

where

$\Omega_D = f(kT/\epsilon_{AB})$, the collision integral for diffusion of A into B

Equation 13 was for component A diffusing through stagnant B.
For equimolar counterdiffusion, i.e. A→B, and A←B such that $N_A = -N_B$.

$$\frac{N_A}{A} = \frac{D_v \rho_m}{B_T}\ (y_{Ai}-y_A) \qquad (17)$$

Equation 13 and 17 are for diffusion only. Where convection is involved,

$$\frac{N_A}{A} = k\ (y_{Ai}-y_A) \qquad (18)$$

where k is a function of the physical setup, such as

$$\frac{kD\bar{M}}{\rho D_v} = \emptyset\ \frac{DG}{\mu}\ ,\ \frac{\mu}{\rho D_v} \qquad (19)$$

$\frac{kD\bar{M}}{\rho D_v}$ = Sherwood number, dimensionless

$\frac{DG}{\mu}$ = Reynolds number, dimensionless

$\frac{\mu}{\rho D_v}$ = Schmidt number, dimensionless

PERMEATION

Gas permeation rates are typically $1.3 \times 10^{-7} \frac{gm}{sec\ cm^2}$

Rate equations for permeability may be written

$$\frac{q}{A} = \frac{P(p_2-p_1)}{t} = \frac{DS(p_2-p_1)}{t} = \frac{DS\pi(y_2-y_1)}{t} \quad (20)$$

$$\frac{q}{A} = \frac{D_c(c_2-c_1)}{t} \quad (21)$$

q = permeation rate in gm/sec (sometimes reported as $cm^3$/sec)

A = cross sectional area for permeation, $cm^2$

t = thickness of film or gasket, cm

$p_2, p_1$ = downstream partial pressure of permeating component and upstream partial pressure, respectively, Pa (often atmsophere, cm. Hg., etc.)

$c_2, c_1$ = downstream and upstream concentration of permeating component, respectively

$y_2, y_1$ = downstream and upstream mole fraction, respectively of permeating component

P = permeability constant, (gm cm)/(sec $cm^2$ Pa) or gm/(sec cm Pa)

D = diffusion constant, $cm^2$/sec (sometimes $cm^2$/min)

S = solubility coefficient, gm/($cm^3$. Pa)

D, S, and therefore P are functions of pressure and temperature.

CBI Permeability Tests

CBI Table 5.2 Neoprene Permeability, t = 2.4 cm, Type II

| Diffusing | Relative Stopper Permeability* (g/day) | |
|---|---|---|
| n-$C_5$ | 0.0267 | |
| n-$C_6$ | 0.0145 | $C_6/C_5$ = 0.543 |
| n-$C_7$ | 0.0100 | |
| n-$C_8$ | 0.0055 | |
| $C_6H_6$ | 0.2011 | |

*g/day is of course equal to q but it is proportional to the permeability P, see Equation 20

It appears that $\frac{\text{Permeability of Benzene}}{\text{Permeability of n-}C_6} = \frac{0.2011}{0.0145} = 13.9$

From Table A-1

| Test | $\frac{g}{cm^2\ sec}$ | Permeant |
|---|---|---|
| 17 | $3.27 \times 10^{-7}$ | $C_6H_6$ |
| 18 | $0.327 \times 10^{-7}$ | n-$C_6$ |
| Lab Permeability Test | $2.95 \times 10^{-7}$ | n-$C_6$ |

Comparing Test 17 and 18 $\frac{\text{Permeability of } C_6H_6}{\text{Permeability of n-}C_6} = \frac{3.27 \times 10^{-7}}{0.327 \times 10^{-7}} = 10$

But compare $\frac{\text{Test 17}}{\text{Lab Permeability Test}} = \frac{(3.27 \times 10^{-7})(0.037)}{(2.95 \times 10^{-7})(0.020)} = 2.0$ more believable

CBI Table 5.2 and Tests 17 and 18 would suggest that the permeability of benzene is greater than 10 times that of hexane. If, however, you look at Lab Permeability Test, it is only a factor of 2, which is more believable.

Literature Data on the Permeability of $C_6H_6$ and n-$C_6$

1. Rogers, C.E., V. Stannett, and M. Szwarc, J. Polymer Sci. 45 61 (1960)

| Benzene | | Hexane | |
|---|---|---|---|
| c | P | c | P |
| 1.8 | 1.77 | 1.58 | 0.821 |
| 4.1 | 3.91 | 3.60 | 2.26 |
| 7.15 | 9.09 | 5.55 | 5.11 |
| | | 8.0 | 11.6 |

Units of c and P are obscure, but comparable.
Note the numbers are the same order of magnitude.

2. Nelson, G.O., G.L. Lum, G.J. Carlson, and J.S. Johnson, AIHA Journal, (42), 217, March 1981.

Table A-2 summarizes data in Nelson paper.

Table A-1. PERMEABILITY OF POLYURETHANE COATED NYLON FABRIC

| Test No. | Fabric Thickness (in) | Fabric Area ($ft^2$) | Length of Taped Seams (in) | Product Type | Average Product Temp. (°F) | Average Vap. Press. (psia) | Vapor Mole. Wt. (lbm/lbmole) | Average Emission Rate (lbm/day) | Correlation Coefficient (-) | Average Permeation Rate ($lbm/ft^2 day$) | Average Permeation Rate ($g/cm^2 sec$) | Notes |
|---|---|---|---|---|---|---|---|---|---|---|---|---|
| 16 | 0.020 | 2.75 | - | C3/nC8 | 59.2 | 7.13 | 45.8 | 0.0612 | 0.838 | 0.0222 | $1.25 \times 10^{-7}$ | |
| 17 | 0.037 | 2.75 | - | C6H6 | 60.5 | 1.22 | 78.1 | 0.159 | 0.996 | 0.0578 | $3.27 \times 10^{-7}$ | |
| 18 | 0.037 | 2.75 | - | nC6 | 60.1 | 1.98 | 86.2 | 0.0158 | 0.663 | 0.00578 | $0.327 \times 10^{-7}$ | |
| 19 | 0.020 | 2.75 | - | C3/nC8 | 53.8 | 3.86 | 46.6 | 0.0652 | 0.703 | 0.0237 | $1.34 \times 10^{-7}$ | |
| 20 | 0.020 | 2.75 | - | C3/nC8 | 48.1 | 3.56 | 46.3 | 0.0808 | 0.806 | 0.0294 | $1.66 \times 10^{-7}$ | |
| 21 | 0.020 | 2.75 | 48 | C3/nC8 | 50.9 | 4.68 | 45.9 | 0.0650 | 0.863 | 0.0236 | $1.33 \times 10^{-7}$ | (1) |
| 22 | 0.020 | 2.75 | - | C3/nC8 | 43.2 | 3.59 | 46.0 | 0.0344 | 0.805 | 0.0125 | $0.706 \times 10^{-7}$ | (1) |
| 23 | 1/16" thk. alum. | | 68 | C3/nC8 | 44.2 | 3.38 | 46.3 | 0.00273 | 0.996 | - | - | |
| Laboratory Permeability Test | | | | | | | | | | | | |
| — | 0.020 | 0.467 | - | nC6 | 74.8 | 1.85 | 86.2 | 0.0244 | — | 0.0522 | $2.95 \times 10^{-7}$ | |

Notes: (1). Aluminum backed duct tape was used on all taped seams.

Table A-2. COMPARISON OF PERMEABILITY OF ALIPHATIC HYDROCARBONS AND BENZENE

| Glove no. | Solvent[A] $n\text{-}D_5$ BR | $n\text{-}D_5$ P | $n\text{-}C_6$[F] BR | $n\text{-}C_6$ P | $C_6H_{12}$ BR | $C_6H_{12}$ P | $C_6H_6$ BR | $C_6H_6$ P | $P_{C_6H_6}/P_{n\text{-}C_6}$ | Glove Comp. |
|---|---|---|---|---|---|---|---|---|---|---|
| 1 | 0.4 | 400 | - | 220 | 1.6 | 100 | 0.1 | 250 | 1.1 | PE |
| 2 | 3.2 | 70 | - | 38 | 10 | 28 | 4.0 | 50 | 1.3 | PE |
| 3 | 0.8[E] | 1100[E] | - | 600[E] | 1.6 | 500 | 0.5[B] | 3500[B] | 5.8 | PVC |
| 4 | 0.8[E] | 810[E] | - | 440[E] | 2.2[D] | 340[D] | 0.4 | 4100 | 9.3 | PVC |
| 5 | 9.2 | 100 | - | 54 | 16 | 100 | 2.2 | 1500 | 28 | PVC |
| 6 | 2.4[D] | 250[D] | - | 140[D] | 5.6 | 200 | 2.2[B] | 1600[B] | 11 | PVC |
| 7 | 0.8[E] | 720[E] | - | 390[E] | 2.0[D] | 310[D] | 0.1[D] | 4700[B] | 12 | PVC |
| 8 | 0.8[E] | 1600[E] | - | 870[E] | 0.8[D] | 450[D] | 0.3[D] | 3600[D] | 4.1 | PVC |
| 9 | 0.9 | 1600[E] | - | 870[E] | 2.4 | 300 | 0.1[D] | 4900[D] | 5.6 | PVC |
| 10 | 0.7 | 5700 | - | 3100 | 1.7 | 1500 | 1.5 | 5600 | 1.8 | SRL |
| 11 | 1.7 | 2700 | - | 1500 | - | 10 | 2.2 | 3200 | 2.1 | NRL |
| 12 | 3.6 | 1800 | - | 980 | 8.0 | 1300 | 3.0 | 2600 | 2.7 | NRL |
| 13 | 4.0 | 1800 | - | 980 | 5.0 | 1400 | 3.0 | 2800 | 2.9 | N/L |
| 14 | 1.6 | 2300 | - | 1200 | - | - | 5.2 | 2000 | 1.7 | NRL |
| 15 | 20 | 21 | - | 11 | 72 | 100 | 4.8 | 1800 | 163 | NEL |
| 16 | 65 | 10 | - | 5 | 700 | <10 | 11.1 | 1000 | 200 | NEL |
| 17 | 38 | 16 | - | 9 | 29 | 100 | 16 | 800 | 89 | NEL |
| 18 | 6.4 | 25 | - | 14 | - | - | 1.2 | 950 | 68 | NEL |
| 19 | >60 | <2 | - | <1 | - | - | 16 | 1100 | >1000 | NEL |

(continued)

Table A-2. Concluded

| Glove no. | Solvent[A] n-$D_5$ BR | n-$D_5$ P | n-$C_6$[F] BR | n-$C_6$ P | $C_6H_{12}$ BR | $C_6H_{12}$ P | $C_6H_6$ BR | $C_6H_6$ P | $P_{C_6H_6}/P_{n\text{-}C_6}$ | Glove Comp. |
|---|---|---|---|---|---|---|---|---|---|---|
| 20 | 6.8 | 24 | - | 13 | 9.6 | 70 | 24 | 300 | 23 | NEL |
| 21 | >60 | <2 | - | <1 | - | - | - | - | - | NEL |
| 22 | >60 | <2 | - | <1 | >60 | <10 | 63 | 400 | >400 | NIR |
| 23 | >60 | <2 | - | <1 | >60 | <1 | 19 | 850 | >850 | NIR |
| 24 | >60 | <2 | - | <1 | >60 | <1 | 46 | 510 | >510 | NIR |
| 25 | 5.6[D] | 10[D] | - | 5 | >60 | <10 | 44 | 1300 | 260 | ANR |
| 26 | 3.5 | 1800 | - | 980 | 9.6 | 1100 | 3.7 | 2200 | 2.2 | NR |
| 27 | 5.2 | 1600 | - | 870 | 18 | 800 | 7.4 | 1600 | 1.8 | NR |
| 28 | - | - | - | - | >60 | <1 | 9.0 | 1100 | - | NIR |

[A]All breakthrough curves exhibit Type A behavior except where noted by G, C, D, or E.

[B]Type B curve (see attached).

[C]Type C curve.

[D]Type D curve.

[E]Type E curve.

[F]Values for n-$C_6$ = (values for $nC_5$ x 0.543). These are estimated values.

[BR]Breakthrough time, min.

[P]Permeation rates $\mu g/(min \cdot cm^2)$

---

ANR - Acrylonitrile rubber; NR - Natrual rubber; PE - Polyethylene; PVC - Polyvinyl chloride; SRL - Surgical rubber latex; NRL - Natural rubber latex; N/L - Neoprene/rubber latex blend; NEL - Heoprene latex; and NIR - Nitrile rubber

# APPENDIX B

## DIFFUSIVITY CALCULATIONS

CBI Table 5.3. Series 4 (Brass stopper) At $70^{o}F$ (1.0 atm)(= $21.11^{o}C$ = $294.26^{o}K$)

Use Equation 14

Table B-1 gives physical constants used in the following calculations.

For Benzene

$$D_v = \frac{0.01498\ T^{1.81}\left(\frac{1}{M_A} + \frac{1}{M_B}\right)^{0.5}}{p\left(T_{cA}T_{cB}\right)^{0.1405}\left(V_{cA}^{0.4}+V_{cB}^{0.4}\right)^2}$$

For air

$T_c = (154.4)(126.2) = 139.6K$

$V_c = 1/8(V_{ci}^{1/3}+V_{cj}^{1/3})^3 = 1/8\ [(74)^{1/3}+(90)^{1/3}]^3 = 81.7$

$D_v$, Benzene into air

$$D_v = \frac{0.01498\ (294.26)^{1.81}\ \left(\frac{1}{78.108} + \frac{1}{29.87}\right)^{0.5}}{\left(\frac{748.8}{760}\right)[(139.6)(562.1)]^{0.1405}[(81.7)^{0.4} + (260)^{0.4}]^2}$$

$D_v = 0.0879\ cm^2/sec$

Antonine Eq. $\log_{10}P = A - \frac{B}{t+C}$

| | | | | $21.1^{o}C$ | |
|---|---|---|---|---|---|
| | A | B | C | $P_t^o$, mm | $y_{Ai}$ |
| Benzene | 6.97025 | 1241.95 | 223.781 | 79.40 | 0.1045 |
| Hexane | 6.9130 | 1187.8 | 225.947 | 127.4 | 0.1676 |

Molecular Diffusion in a CBI Test I Apparatus

Table B-1. PHYSICAL CONSTANTS

| | $T_c$, $^oK$ | $p_c$, atm | $V_c$ L/gmole | $z_c$ | M.W., g/gmole | σ dynes/cm 20°C | σ dynes/cm 30°C |
|---|---|---|---|---|---|---|---|
| Benzene, $C_6 H_6$ | 562.1 | 48.6 | 0.260 | 0.274 | 78.108 | 28.85 | 27.56 |
| Hexane, n-$C_6 H_{14}$ | 507.9 | 29.92 | 0.368 | - | 86.172 | 18.43 | - |
| Oxygen, $O_2$ | 154.4 | 49.7 | 0.074 | 0.290 | 16.000 | - | - |
| Nitrogen, $N_2$ | 126.2 | 33.5 | 0.090 | 0.291 | 14.008 | - | - |

Equation 13

$$\frac{N_A}{A} = \frac{D_v \rho_m}{B_T} \ln \frac{1-y_A}{1-y_{Ai}}$$

Assume: $y_A = 0$

$$\frac{N_A}{A} = \frac{D_v \text{ cm}_2/\text{sec } \rho_m \frac{\text{gmole}}{\text{cm3}}}{B_T \text{ cm}} \ln \frac{1-y_A}{1-y_{Ai}}$$

$$= \text{gmole}/(\text{cm}^2 \text{ sec})$$

For the Test Apparatus I Diffusion tube = 2.5" long = 6.35 cm

$$pv = nRT = \frac{W}{M} RT$$

$$\rho_m = \frac{PM}{RT} = \frac{\text{atm}}{\frac{\text{cc atm K}}{\text{gmole K}}} = \frac{\text{gmole}}{\text{cc}}$$

$$\rho_m = \frac{(748.8 \text{ mm}/700)}{(82.06 \frac{\text{cc atm}}{\text{gmole } ^oK})(294.26^oK)} = 4.076 \times 10^{-5} \text{ gmole/cc}$$

$$N_A = \frac{(A)(D_v)(\rho_m)}{B_T} \ln (1/1-y_{ai})$$

For Benzene:

$$N_A = \frac{(0.1642 \text{ cm}^2)(0.0879 \text{ cm}^2/\text{sec})(4.076 \times 10^{-5} \text{ gmole/cm}^3)}{6.35 \text{ cm}} \ln [1/(1-0.1045)]$$

$$N_A = 1.023 \times 10^{-8} \text{ gmoles/sec}$$

Convert to grams/day

$N_A = 1.023 \times 10^{-8}$ gmole/sec x 78.108 gm/gmole x 60 sec/min x 60 min/hr x 24 hrs/day

Benzene

$N_A = 0.0690$ gm/day  cf. 0.069 gm/day from Table 5.3 of CBI report page 99

For Hexane (into air)

$$D_v = \frac{0.01498\ T^{1.81}\ (1/M_A + 1/M_B)^{0.5}}{P(T_{cA}T_{cB})^{0.1405}(V_{cA}^{0.4} + V_{cB}^{0.4})^2}$$

$$= \frac{0.01498\ (294.26)^{1.81}\ (1/86.172 + 1/28.97)^{0.5}}{(7488/760)[(139.6)(507.9)]^{0.1405}[(81.7)^{0.4} + (368)^{0.4}]^2}$$

$$D_v = 0.07392\ cm^2/sec$$

$$N_A = \frac{(0.1642\ cm^2/sec)(0.07392\ cm^2/sec)(4.076 \times 10^{-5}\ gmole/cm^3)}{6.35\ cm} \ln [1/(1-0.1676)]$$

$$= 1.429 \times 10^{-8}\ gmole/sec$$

Now convert to gm/day

$N_A$ - 1.429 x $10^{-8}$ gmole/sec x 86.172 gm/gmole x 60 sec/min x 60 min/hr x 24 hr/day

$N_A$ = 0.1064 gm/day  cf. CBI Table 5.3  0.126 gm/day
I calculate  (0.120 gm/day)

Theoretical value

CBI calculation  18.4% hi
McA calculation  12.8% hi

With Series 4, Type 3, there is no way to estimate the length of the diffusion path for Type III stopper

Now lets check out Test Series 1, 2, and 3

T = 21.11°C

P = 750.1 mm Hg

$B_T$ = 2" long (= 5.08 cm)

$$A = \frac{\pi[(11/64\ in) \times 2.54\ cm/in]^2}{4}$$

$$= 0.1497\ cm^2$$

Estimate $v_c$ for i-$C_8$, 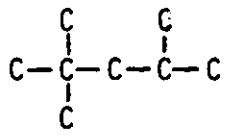 by Lyderson Method see CPPI, p. 88

| | | $v_{ci}$ |
|---|---|---|
| 5 (–$CH_3$) | = 5(55) | = 275 |
| 1 (–C–) | | = 41 |
| 1 (–CH) | | = 51 |
| 1 (–$CH_2$) | | = 55 |
| 2,2,4 trimethylpentane | $v_c$ | = 422 $cm^3$/gmole |

For Hexane and Benzene $(D_v)_{\text{series 1,2,3}} = (D_v)_{\text{series 4}} \times 748.8/750.1$

For Pentane

$$D_v = \frac{0.01498\ (294.26)^{1.81}\ (1/72.146 + 1/28.97)^{0.5}}{(7501./760)[(4698)(139.6)]^{0.1405}\ [(81.7)^{0.4} + (311)^{0.4}]^2}$$

$= 0.0833\ cm^2/sec$

For Heptane

$$D_v = \frac{(0.01498)(294.26)^{1.81}\ (1/100.198 + 1/28.97)^{0.5}}{(750.1/760)[(540.16)(139.6)]^{0.1405}\ [(81.7)^{0.4} + (426)^{0.4}]^2}$$

$= 0.0666\ cm^2/sec$

For Octane

$$D_v = \frac{(0.01498(294.26)^{1.81}\ (1/114.224 + 1/28.97)^{0.5}}{750.1/760[(569.4)(139.6)]^{0.1405}\ [(81.7)^{0.4} + (486)^{0.4}]^2}$$

$= 0.0607\ cm^2/sec$

For iso-Octane

$$D_v = \frac{0.01498(294.26)^{1.81}\ (1/114.224 + 1/28.97)^{0.5}}{750.1/760[(567.1)(139.6)]^{0.1405}\ [(81.7)^{0.4} + (422)^{0.4}]^{0.5}}$$

$= 0.0655\ cm^2/sec$

Vapor Pressure

At $70^oF$

| | | | $y_{Ai}$ | $\ln 1/(1-y_{Ai})$ |
|---|---|---|---|---|
| $C_5$ | = 8 psia | (= 414 mm) | 0.545 | 0.78746 |
| $C_6$ | = 2.6 | (= 134 mm) | 0.176 | 0.19358 |
| $C_7$ | = 0.7 | (= 36.2 mm) | 0.048 | 0.04919 |
| $C_8$ | = 0.205 | (= 10.6 mm) | 0.014 | 0.01410 |
| $iC_8$ | = | (≐ 42 mm) | 0.055 | 0.05657 |
| Previous Calculation | | | | |
| $n\text{-}C_6$ | | | 0.1676 | 0.18344 |
| $C_6H_6$ | | | 0.1045 | 0.11037 |

Read from Van Winkle, M., "Distillation," McGraw Hill Book Co., New York (1967) p. 665.

$$N_A = \frac{(A)(D_v)(\rho_m)}{B_T} \ln 1/(1-y_{Ai})$$

$$\rho_m = \frac{750.1/760}{(82.06)(294.26)} = 4.087 \times 10^{-5}\ gmole/cm^3$$

$$N_A = \frac{(0.1497)(4.087 \times 10^{-5})}{(5.08)} (D_v) \ln [1/(1-y_{Ai})] (60)(60)(24)(M) \quad in\ g/day$$

$= 0.10405824\ \ D_v \ln [1/(1-y_{Ai})]\ M$

For Pentane $C_5$ $\quad N_A = 0.4925$ gm/day

See Table B-2 for the rest of the values.

Table B-2. DIFFUSION CALCULATIONS, TYPE I APPARATUS

| Hydrocarbons | Gross diffusion (g/day) | $M_A$ (g/gmole) | $T_c$ K | $v_c$ cc/gmole | $(D_v)_{70^oF}$ $cm^2/sec$ | $N_A$, Theoretical diffusion in tube gm/day | $\Delta$ g/D |
|---|---|---|---|---|---|---|---|
| n-$C_5$ $H_{12}$ | 0.6530 | 72.146 | 469.8 | 311 | 0.0833 | 0.4925 | 0.1605 |
| n-$C_6$ $H_{14}$ | 0.1762 | 86.172 | 507.9 | 368 | 0.0738 | 0.1214 | 0.0548 |
| n-$C_7$ $H_{16}$ | 0.0432 | 100.198 | 540.16 | 426 | 0.0666 | 0.0342 | 0.0090 |
| n-$C_8$ $H_{18}$ | 0.0120 | 114.224 | 569.4 | 486 | 0.0607 | 0.0102 | 0.0018 |
| i-$C_8$ $H_{18}$ | 0.0482 | 114.224 | 567.1 | 422 | 0.0655 | 0.0440 | 0.0042 |
| $C_6$ $H_6$ | 0.1842 | 78.108 | 562.1 | 260 | 0.0876 | 0.0786 | 0.1056 |

Table B-3. COMPARISON OF STOPPER PERMEABILITY/DIFFUSION TEST, SERIES 1, 2, and 3
(cf. Table 5.2, CBI, p. 98)

| Hydrocarbon | Cum. Gross Diff. g/D | Cum. Gross Diff. cv % | Δ Gross Diff. g/D | Δ Gross Diff. cv % | Cum. Stopper Perm. g/D | Cum. Stopper Perm. cv % | Δ Stopper Perm. g/D | Δ Stopper Perm. cv % | Net Tube Diff. cum g/D | Net Tube Diff. Δg/ΔD g/D | Theor. tube Diff. g/D |
|---|---|---|---|---|---|---|---|---|---|---|---|
| n-Pentane | 0.6540 | 4.9 | 0.6640[a] | 4.4[a] | 0.0266 | 13.9 | 0.0357 | 11.6 | 0.6274 | 0.6283 | 0.4925 |
| n-Hexane | 0.1762 | 3.3 | 0.1803[a] | 2.7[a] | 0.0146 | 23.0 | 0.0205 | 9.2 | 0.1616 | 0.1598 | 0.1214 |
| n-Heptane | 0.0430 | 5.2 | 0.0483 | 9.7 | 0.0088[b] | - | 0.0133[b] | - | 0.0342 | 0.0350 | 0.0342 |
| n-Octane | 0.0120 | 8.3 | 0.0154[a] | 10.4[a] | 0.0054 | 38.4 | 0.0091 | 14.1 | 0.0066 | 0.0063 | 0.0102 |
| i-Octane | 0.0480 | 7.6 | 0.0506[a] | 7.1[a] | - | - | - | - | - | - | 0.0440 |
| Benzene | 0.1842 | 2.7 | 0.2486 | 5.2 | 0.2012 | 8.0 | 0.2265 | 6.0 | -0.0170 | 0.0221 | 0.0786 |

[a]Used last two Δg/ΔD values for each flask.

[b]Graphical interpolation with n-$C_6$, n-$C_7$, and n-$C_8$ data, see Figure B-1.

The stopper permeability tests are given in Table B-3. These data include most of the data in the CBI Table 5.2 (p. 98), but corrected by using the data in CBI Appendix F. The loss ratio listed under Cumulative Gross Diffusion were calculated as follows:

1. A plot of cumulative weight change vs. test duration was plotted.

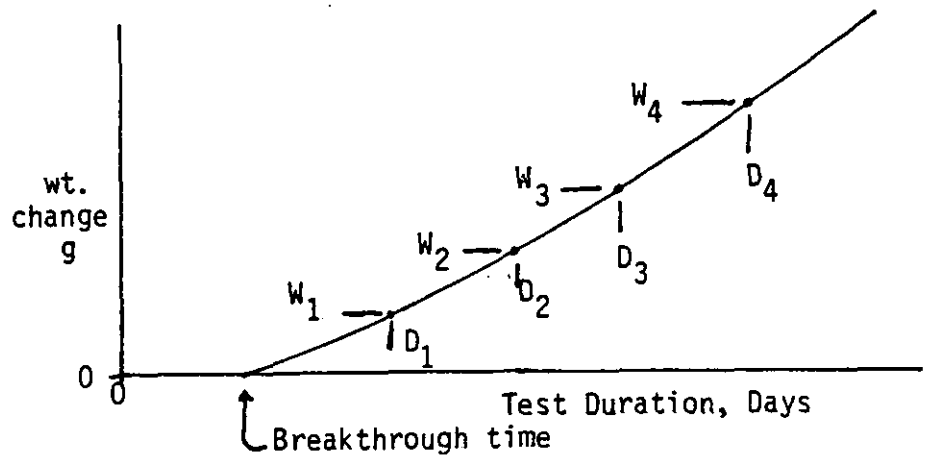


2. For cumulative gross diffusion

$(g/D)_1 = W_1/D_1$

$(g/D)_2 = W_2/D_2$

$(g/D)_3 = W_3/D_3$

3. For $\Delta$ gross diffusion

$(\Delta g/\Delta D)_1 = (W_1-0)/(D_1-0)$

$(\Delta g/\Delta D)_2 = (W_2-W_1)/(D_2-D_1)$

$(\Delta g/\Delta D)_3 = (W_3-W_2)/(D_3-D_2)$

The latter Method 3 is the more appropriate method, since the permeation rate (or loss rate) is a derivative quantity, a rate. The results from Appendix F show that in every case, the permeation followed permeation behavior A or B, shown in Figure B-2.

The cumulative gross diffusion figures in Table B-3 includes diffusion through the open shell tube (Type I apparatus, Figure 5.1 page 96, CBI Report) and permeation through the neoprene stopper. The cumulative stopper permeability figures in Table B-3 were calculated from data in CBI Appendix F for a Type II apparatus (Figure 5.1 CBI Report), and were intended to measure permeability of the stopper itself.

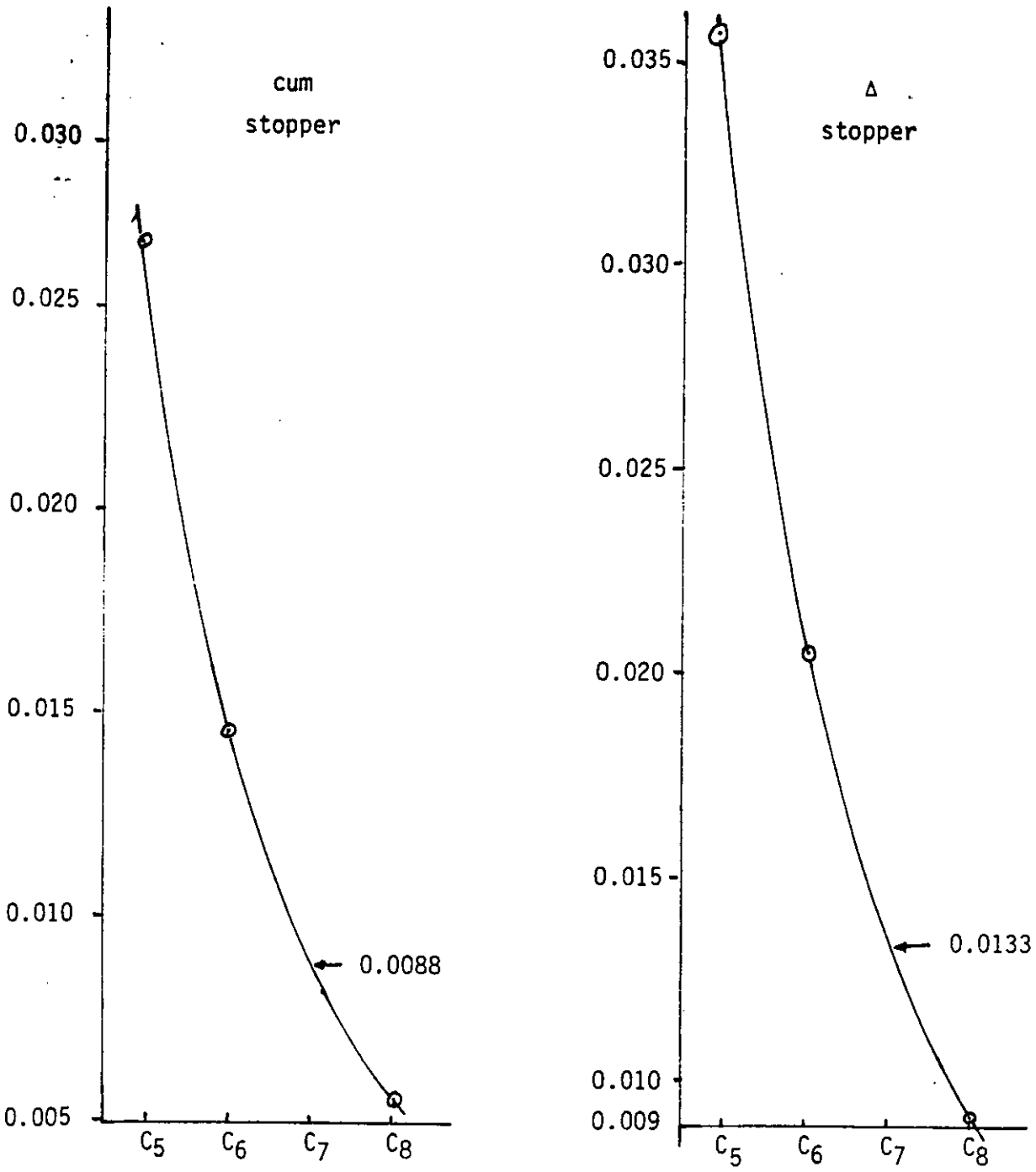


Figure B-1. Graphical interpolation of stopper permeability.

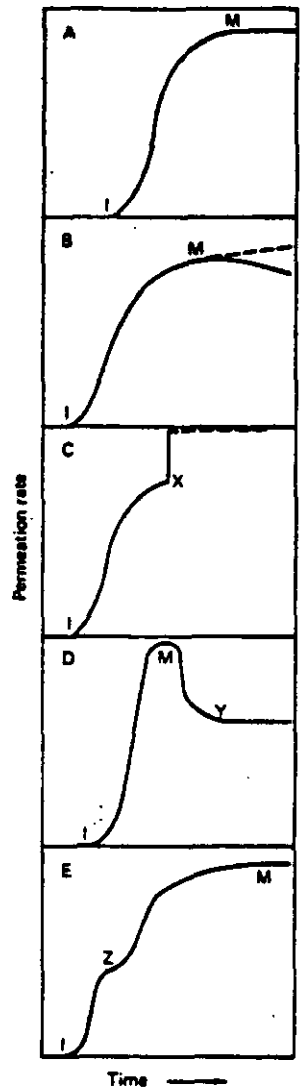


Figure B-2. Five types of glove permeation behavior.

The data listed as "Net Tube Diffusion" in Table B-3 is the difference between "cumulative gross diffusion" and "cumulative stopper permability."

Cum. Net Tube Diffusion = (Cumulative Gross Diffusion)-(Cumulative Stopper Permerability) or

$\Delta g/\Delta D$ Net Tube Diffusion = ($\Delta$ Gross Diffusion)-($\Delta$ Stopper Permeability)

The net tube diffusion figures may be compared with the theoretical tube diffusion column in Table B-3. The latter figures were calculated theoretically assuming 70°F, atmospheric pressure 750.1 mm Hg and the room concentration of the diffusing component equal to zero. Note that the theoretical diffusion rates are comparable to the measured ones (maximum of 27.6% different for n-$C_5$) with the exception of benzene. For benzene, the measured stopper permeability rate is about three times the diffusion rate. Further, it appears that an unsteady state obtains, so that point M on curve A, Figure B-2 has not yet been reached for benzene. This is undoubtedly due to the high solubility parameter for benzene in neoprene.

The CV (in %) figures listed in Table B-3 give values of $s_x/\overline{X}$ (in %) for the five flasks used for each test. For these CV values, the last value for loss rate was used in each case, except for those indicated as footnote "a." The latter values appeared to level off (Point M, Chart A, in Figures B-2), or turndown (Point M, Chart B, Figures B-2), so the last two values of $\Delta g/\Delta D$ were used for each flask. The leveling off indicated: (a) Point M in Figures B-2 had been reached, or (b) successive values of $\Delta g$ were so small as to be equal to or less than the experimental error. While CV values for gross diffusion data were about comparable for each hydrocarbon (comparing CV for cum. and $\Delta$ gross diffusion rates). For the "cum. stopper permeabilities" and the "$\Delta$ stopper permeabilities" there was a considerable improvement of CV for the $\Delta$ stopper permeabilities.

Note that the cum. net tube diffusion for benzene is negative, and that for the $\Delta g/\Delta D$ method, the net tube diffusion is positive, although about 1/3 of the theoretically calculated value. These figures emphasize the fact that for the benzene, steady state has not been reached. It further confirms the fact that the $\Delta g/\Delta D$ method of calculation is superior to the cumulative method of calculation.

# APPENDIX C

# DECK FITTING CALCULATIONS

## Table C-1. IFR DECK FITTING TESTS, DIFFUSING HEXANE

| Test No. | $(WA/A)_A$ ($gm/cm^2$ day) | $\frac{(WA/A)_A}{(WA/A)_D}$ | Description |
|---|---|---|---|
| 3 | 11.597 | 15.2 | 1/2" gap, 1 1/2" pipe* |
| 4 | 0.6172 | 0.81 | ≈8" dia. hole, slotted sample well |
| 5 | 4.119 | 5.39 | 1/8" gap around solid pipe, 8" pipe |
| 6 | 1.728 | 2.26 | 1" i.d. well straight diffusion |
| 8 | 13.34 | 17.4 | 1/2" gap, double channels |
| 12 | 21.74 | 28.4 | 1/8" gap around double channels |
| 13 | 4.037 | 5.28 | 1/8" gap around a circle, 22.5" drum |
| 14 | 1.723 | 2.25 | 10% area well protected |
| 15 | 24.27 | 31.7 | 1/8" gap around double channels |

General Notes:

1. Test 4 looks inordinately low. Should be the highest.

2. Note 1/2" gaps: Runs 3 ; $(WA/A)_A/(WA/A)_D$ = 15.2
   8 ; $(WA/A)_A/(WA/A)_D$ = 17.4

3. Note 1/8" gaps: Runs 5 ; $(WA/A)_A/(WA/A)_D$ = 5.39 Circular pipe
   12 ; $(WA/A)_A/(WA/A)_D$ = 28.4 Double channels
   13 ; $(WA/A)_A/(WA/A)_D$ = 5.28 Circular drum
   15 ; $(WA/A)_A/(WA/A)_D$ = 31.7 Double channels

4. Straight diffusion well protected
   6 ; $(WA/A)_A/(WA/A)_D$ = 2.26 1" i.d. well
   14 ; $(WA/A)_A/(WA/A)_D$ = 2.25 Iris closure funnel

*Maybe this should have been done on a 0.083" circumferential gap around a 1 1/2" pipe.

Environ. Sci. Technol. 1982, 16, 726–728

# Calculation of Evaporative Emissions from Multicomponent Liquid Spills

Peter J. Drivas*

Environmental Research & Technology, Inc., Concord, Massachusetts 01742

■ A theoretical formulation is presented that enables the calculation of the evaporation rates of individual compounds in a multicomponent liquid mixture, as a function of time from a spill. The calculation of evaporation rates is based on conventional mass transfer theory and the assumption of a well-mixed liquid phase. The total evaporation rate, the liquid-phase composition, and the gas-phase composition can all be explicitly calculated as a function of time from the spill. Comparison of the theoretical results with experimental data on oil spill evaporation showed good agreement.

## *Introduction*

For calculation of the air quality impact of volatile liquid spills, knowledge of the time-dependent evaporative emission rate is a necessary input for air quality simulation models. In a multicomponent liquid spill, the evaporative emission rate for each individual compound, as well as the total evaporation rate, may have to be estimated. The emission rates of individual components are necessary as input for both photochemical air quality modeling, which requires emission rates by hydrocarbon species class (*1*), and modeling for toxicity, hazard, or odor impacts of individual compounds from oil spills or hazardous material spills. Several studies have shown that evaporation is the primary mechanism of low-carbon-number hydrocarbon loss in an oil spill (*2*, *3*).

A relatively simple theoretical formulation is presented to calculate individual evaporation rates in a multicomponent liquid spill based on conventional convective mass transfer theory. The necessary inputs for the calculation are (1) initial mass of spill, (2) initial liquid composition, (3) spill area, (4) ambient air temperature, (5) windspeed, and (6) atmospheric stability. The mass transfer coefficient is based on an empirical fit to a solution of the steady-state atmospheric diffusion equation with power-law vertical velocity and eddy diffusivity profiles. Because of the mass transfer formulation, the analysis applies primarily to liquids with boiling points higher than ambient temperatures and does not necessarily apply to spills of liquified gases, where evaporation may be limited by heat transfer.

## *Evaporation Theory*

The problem is to derive an expression for the time-dependent evaporation rate in a multicomponent liquid system. Application of the standard mass transfer rate equation for evaporation (*4*) to each component, with the assumptions of an ideal solution, a well-mixed liquid phase, and negligible atmospheric concentrations yields

$$dn_i/dt = -kp_i^s n_i \tag{1}$$

where

$$k = k_G A/n_T \tag{2}$$

and where $dn_i/dt$ is the loss rate of moles of liquid component $i$ per unit time, $p_i^s$ is the saturation (pure) vapor pressure of component $i$, $k_G$ is the mass transfer coefficient (mol m$^{-2}$ atm$^{-1}$ h$^{-1}$), $A$ is the liquid surface area (m$^2$), and $n_T$ is the total moles of liquid.

The above formulation requires the further assumption that the ratio $n_T/A$ remains approximately constant; thus, the coefficient, $k$, can be considered a modified mass transfer coefficient, with units of atm$^{-1}$ h$^{-1}$. Equation 1 is essentially identical with that used by Harrison et al. (*5*) in their experimental study of oil spill evaporation, and it presents the intuitive explanation that the evaporation loss of a compound is proportional to its vapor pressure and the amount of the compound remaining. The assumption that $n_T/A$ remains constant is more appropriate for spills on land or close to shore than on open water, because oil spills on open water normally increase in area with time.

The solution of eq 1 is very straightforward:

$$n_i = n_i^0 e^{-kp_i^s t} \tag{3}$$

where $n_i^0$ is the initial number of moles of liquid component $i$. Thus, for a one-component system, the evaporation rate expression is very simple.

For a multicomponent liquid system, the individual evaporation rates must be summed to obtain a total evaporation rate. Summing eq 3 over all compounds, taking a derivative to obtain a total emission rate (mass/time), and using Raoult's law yield

$$\frac{dm_T}{dt} = -km_T^0 \sum_{i=1}^{N} [x_i^0 p_i^s M_i e^{-kp_i^s t}] / \sum_{i=1}^{N} x_i^0 M_i \tag{4}$$

where $dm_T/dt$ is the total evaporative emission rate (mass/time), $m_T^0$ is the total initial mass of evaporable liquid, $N$ is the number of components, $x_i^0$ is the initial liquid mole fraction of component $i$, and $M_i$ is the molecular weight of component $i$.

Similarly, combining eq 3 and Raoult's law and summing over all components yield

$$p_i = x_i^0 p_i^s e^{-kp_i^s t} / \sum_{i=1}^{N} x_i^0 e^{-kp_i^s t} \tag{5}$$

where $p_i$ is the partial pressure of component $i$ as a function of time.

Equations 4 and 5 define the total evaporation loss rate and vapor composition as a function of time from the spill. The initial mole fraction $x_i^0$ can be derived from a knowledge of the initial liquid phase composition or can be estimated from a known vapor-phase composition over the liquid by using Raoult's law. An excellent summary of evaporative hydrocarbon emissions from a variety of sources is presented by the U.S. Environmental Protection Agency (*6*).

The mass transfer coefficient, $k_G$, in eq 2 is theoretically a function of windspeed and atmospheric stability (*7–9*). Current formulations for $k_G$ are based primarily on the work of Sutton (*7*), who solved the steady-state atmospheric diffusion equation over a liquid pool with a power-law vertical velocity profile and a corresponding power-law eddy diffusivity profile. His resulting expression for $k_G$ as a function of wind velocity, atmospheric stability, and liquid pool dimension has been used by Mackay and Matsugu (*8*) and Fleischer (*9*) to model evaporation rates from liquid spills. Liss and Slater (*10*) derived an average

* To whom correspondence should be addressed at: Energy Resources Company/California, 3344 North Torrey Pines Court, La Jolla, California 92037.

C-2

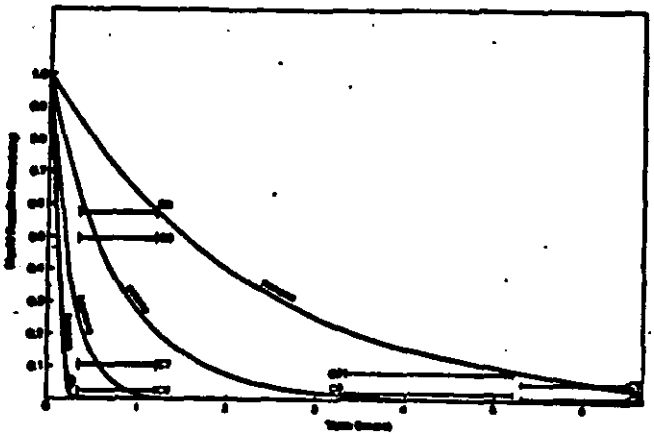

Figure 1. Comparison of single-component theoretical calculations (solid curves) with experimental data (horizontal bars) from a small oil spill (3). The experimental horizontal bars indicate the extent of time-averaged sample collection.

evaporation rate appropriate for the open sea surface but did not consider the effects of windspeed, stability, or liquid area.

The most detailed work has been that of Mackay and Matsugu (8), who used Sutton's theory for neutral atmospheric stability to analyze experimental cumene evaporation and formed the correlation

$$k_G = 0.0292u^{0.78}d_0^{-0.11}Sc^{-0.67}/(RT) \qquad (6)$$

where $u$ is windspeed (m/h), $d_0$ is the spill equivalent diameter (m), $Sc$ is the gas-phase Schmidt number (the ratio of kinematic viscosity to molecular diffusivity), $R$ is the gas constant ($8.206 \times 10^{-5}$ atm m$^3$ mol$^{-1}$ K$^{-1}$), and $T$ is temperature (K). This expression can be easily used to calculate the modified mass transfer coefficient, $k$, in eq 4 and 5 during neutral stability conditions. Alternatively, $k$ can be estimated empirically from experimental evaporation rates of individual compounds with eq 3.

### *Comparison of Theory with Experimental Data*

For comparison with measured evaporation data, the theoretical analysis in eq 6 and 2 will be used to calculate a typical value of the modified mass transfer coefficient, $k$. With a windspeed of 5 m/s, an effective spill diameter of 100 m, a Schmidt number of 2.7, and a temperature of 20 °C, eq 6 results in a value of $k_G$ = 780 mol m$^{-2}$ atm$^{-1}$ h$^{-1}$. To estimate an approximate value of $n_T/A$ to use in eq 2, it will be assumed that a spill has a thickness of 0.001 m and the evaporable liquid has an average molecular weight of 134 g/mol and an average specific gravity of 0.6. These values result in $n_T/A$ = 4.5 mol/m$^2$; Harrison et al. (5) used 5 mol/m$^2$ in the analysis of their experimental results. The resulting value of $k$, from eq 2, is about 170 atm$^{-1}$ h$^{-1}$.

This value of $k$ can be compared to measured evaporation rates of individual compounds from experimental oil spills, by using eq 3. Johnson et al. (3) present experimental data on the approximate evaporation rates of $C_5$–$C_9$ hydrocarbons in four actual oil spills on water. With the use of eq 3 and the appropriate vapor pressures, empirical values of $k$ were derived. They ranged from 40 to 500 atm$^{-1}$ h$^{-1}$ (a typical value was 150 atm$^{-1}$ h$^{-1}$). Somewhat higher values of $k$ would be expected because of the relatively high windspeeds (4–14 m/s) during the experiments. Thus, empirical estimates for the modified mass transfer coefficient agree reasonably well with a theoretical calculation using eq 6 and 2. With the use of $k$ = 150 atm$^{-1}$ h$^{-1}$, the theoretical curves using eq 3 are compared with experimental data from one oil spill in Figure 1.

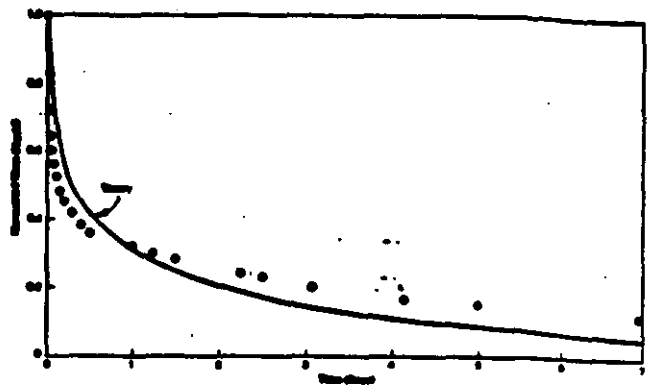

Figure 2. Comparison of multicomponent theoretical calculations (solid curve) with experimental data points (⊙) from long-term crude oil evaporation (11).

The multicomponent evaporation theory presented in eq 4 was compared with experimental data on crude oil evaporation in a wind tunnel. In these experiments, Matsugu (11) monitored the weight loss of crude oil over time periods of several days. Data points from Figure 22 of Matsugu (11) are reproduced in Figure 2 (with the assumption that 50% of the total weight of the oil was evaporable); these data were taken at 20 °C and a windspeed of 4.1 m/s. The experimental conditions resulted in a calculated value of $k$ = 35 atm$^{-1}$ h$^{-1}$, assuming an evaporable oil mass of 250 g and an average molecular weight of 130 g/mol. The initial liquid composition, although not stated, was assumed to be the average crude oil composition derived from the gas-phase composition presented in Kilgren and Hecht (12). From eq 4, the calculated evaporation loss is compared with the experimental data in Figure 2 and shows reasonably good agreement. The theory overpredicts evaporation after a few days, probably because the remaining oil becomes too viscous for the well-mixed assumption to apply.

### *Conclusions*

A relatively simple theoretical formulation has been presented to calculate the time-dependent evaporation rates of individual components in a multicomponent liquid spill. Equations have been derived to calculate the total evaporation rate, the liquid-phase composition, and the gas-phase composition as a function of time from a spill. So that this theoretical formulation can be used in air quality simulation models, the total emission rate (eq 4) is multiplied by the gas mole fraction (eq 5) for the particular compounds of interest. This results in the time-dependent evaporative emission rate of a particular compound in a multicomponent liquid spill, for use in a toxicity, hazard, or air quality impact evaluation.

### *Acknowledgments*

I thank Su Pan for making the calculations.

### *Literature Cited*

(1) "Procedures for the Preparation of Emission Inventories for Volatile Organic Compounds. Vol. II. Emission Inventory Requirements for Photochemical Air Quality Simulation Models"; U.S. Environmental Protection Agency, Research Triangle Park, NC, 1979; EPA-450/4-79-018.
(2) Williams, G. N.; Hann, R.; James, W. P. Proceedings of the 1975 Conference on Prevention and Control of Oil Pollution, San Francisco, CA, March 25–27, 1975.
(3) Johnson, J. C.; McAuliffe, C. D.; Brown, R. A. "Chemical Dispersants for the Control of Oil Spills"; American Society for Testing and Materials: Philadelphia, PA, 1978; Special Technical Publication 659, pp 141–158.

(4) Foust, A. S.; Wenzel, L. A.; Clump, C. W.; Maus, L.; Andersen, L. B. "Principles of Unit Operations"; Wiley: New York, 1960.
(5) Harrison, W.; Winnik, M. A.; Kwong, P. T. Y.; Mackay, D. Environ. Sci. Technol. 1975, 9, 231–234.
(6) "Volatile Organic Compound (VOC) Species Data Manual", 2nd ed.; U.S. Environmental Protection Agency, Research Triangle Park, NC, 1980; EPA-450/4-80-015.
(7) Sutton, O. G. "Micrometeorology"; McGraw-Hill: New York, 1953.
(8) Mackay, D.; Matsugu, R. S. *Can. J. Chem. Eng.* 1973, *51*, 434–439.
(9) Fleischer, M. T. "Proceedings of the 1980 National Conference on Control of Hazardous Material Spills"; Louisville, KY, May 13–15, 1980.
(10) Lisa, P. S.; Slater, P. G. *Nature (London)* 1974, *247*, 181–184.
(11) Matsugu, R. S. M.S. Thesis, Department of Chemical Engineering and Applied Chemistry, University of Toronto, Toronto, Canada, 1973.
(12) Kilgren, K. H.; Hecht, T. A. Hydrocarbon Emissions During Marine Loading of Crude Oils. 71st Annual Meeting of Air Pollution Control Association, Houston, June 25–30, 1978; paper 78-27.6.

*Received for review September 9, 1981. Revised manuscript received June 14, 1982. Accepted June 29, 1982. The E. C. Jordan Co. and the State of Maine Department of Environmental Protection are thanked for providing financial support.*

# Coal Gasification Solid Wastes: Physicochemical Characterization

**Suk Y. Lee**

Environmental Sciences Division, Oak Ridge National Laboratory, Oak Ridge, Tennessee 37830

■ Physicochemical and morphological characteristics of coal gasification solid wastes produced by three different processes were investigated to assess the potential environmental impacts of disposal of these wastes. The wastes were composed of either calcic or ferruginous aluminosilicate glass with small amounts (1–7%) of magnetic particles. The calcic waste had relatively clean surfaces and a homogeneous matrix composition. The magnetic fraction of the waste was composed of metallic iron particles. The ferruginous wastes were occasionally covered by iron oxide or sulfide coatings. Magnetic particles in one ferruginous waste had immiscible iron oxide and sulfide phases in a silicate matrix. The magnetic fraction of the other waste was composed of iron sulfide particles. Some chalcophile elements displayed an association with the surface coatings and magnetic fractions. The gasification solid wastes were different from each other in almost every aspect as they represent products from extremely diverse process conditions.

Coal conversion technologies are being developed to utilize relatively abundant coal resources for the production of synthetic gas and liquid fuel. Evaluation of the technical, economic, and environmental viability of near commercial-scale gasification demonstration plants is in progress (*1*). Commercial gasification plants will consume vast amounts of coal and produce large volumes of solid wastes, the disposal of which could lead to health, environmental, and land-use problems (*2*). As part of the initial effort to assess the effects of solid waste disposal on the environment, the physicochemical characteristics of the wastes produced by three different pilot plants were investigated.

## *Experimental Methods*

Gasification solid wastes (ash or slag) were obtained from three pilot plants that employed extremely diverse process conditions in terms of process pressure, temperature, redox condition, and reactor-bed type. The name of each individual process waste was coded as waste A, B, and C, because of the proprietary nature of the processes. Waste A was produced by a process using a high-pressure fixed-bed gasifier designed to provide low outlet gas temperature and to maintain the operating temperatures above the melting point of the coal ash at the bottom of the gasifier. As an ash-fluxing agent, crushed limestone was added to remove the ash as a molten slag. Waste B was a bottom ash of a process using a multistage fluidized-bed gasifier. After a series of pyrolysis and gasification stages, the solid waste was produced by a slagging combustor designed to utilized carbon in the residual char as a heat source for the process. The process producing waste C used an entrained-bed type gasifier. This type of gasifier is operated at high temperature with short residence time. The gasifier can process both finely pulverized coal and mineral slurry which contains significant amounts of residual carbon. Wastes collected from each gasifier were water quenched. The pilot gasification plants used Pittsburgh No. 8 (waste A), Illinois No. 5 and 6 (waste B), and Kentucky No. 9/14 (waste C) coal.

About 10 kg of solid wastes from each pilot plant were air-dried for characterization. The samples were mixed thoroughly and quartered. Scoopfuls were taken from each quarter until desired amounts were collected for the different analyses. Duplicate samples were collected for each analysis, and average values for the duplicates are presented in Table I. Physical properties such as bulk density, particle density, and particle size distribution were determined by standard methods (*3*). Ferromagnetic particles in the waste were separated by a horseshoe magnet. Morphology of the wastes was examined by scanning electron microscopy (SEM), and qualitative chemical composition of the surface and the cross-section surfaces of particles was determined by an energy-dispersive X-ray analyzer (EDX) attached to the SEM. A part of the bulk samples and magnetically separated fractions was ground with an agate mortar and used for X-ray diffraction (XRD) and neutron activation analysis (NAA). After acid dissolution of ground samples, selected elements were analyzed by atomic absorption and/or argon plasma atomic emission spectroscopy. Total sulfur and carbon contents were determined with an automatic LECO titrator and carbon combustion train analyzer, respectively.

## *Results and Discussion*

The gasification wastes were composed of grey to brownish-black particles with a wide range of shapes and sizes. The mean particle size of waste A was 1.1 mm, and about 70% of the particles were between 0.5 and 2 mm in diameter. Waste B had the largest mean particle size (4.3 mm), and about 87% of the waste was composed of particle

# APPENDIX D

# PERMEABILITY CALCULATIONS

$$q = \frac{A}{x}(p_1 - p_2)P_o e^{-E/RT} \quad (1)$$

$$= \frac{A}{x}(p_1 - p_2)P \quad (2)$$

$$\frac{q}{A} = \frac{P}{x}(p_1 - p_2) \quad (3)$$

$$\frac{q\rho}{A} = \frac{P}{x}(p_1 - p_2) = Q \quad (4)$$

$q = cm^3/sec$

$\rho = gm/cm^3$

$A = cm^2$

$Q = gm/(sec\ cm^2)$

$x$ = membrane thickness, cm

$P_o$ = permeability at reference temperature $T_o$

$P$ = permeability constant, $(gm\ cm)/(cm^2\ sec\ atm)$

Let $R \equiv (x/P)$ (5)

$$Q = \frac{1}{R}(p_1 - p_2) \quad (6)$$

Single layer permeation.

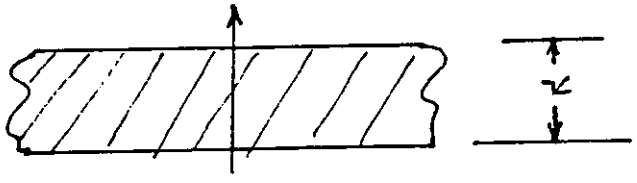


For three layers.

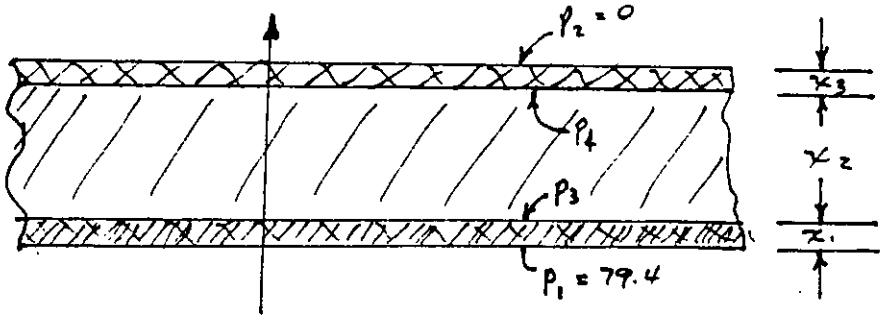

For the composite membrane

$$Q = \frac{(p_1-p_2)}{R_o} \tag{7}$$

$$(p_1-p_2) = (p_1-p_3)+(p_3-p_4)+(p_4-p_2) \tag{8}$$

$$QR_o = Q(R_1) + Q(R_2) + Q(R_3) \tag{9}$$

$$R_o = (x_1/P_1) + (x_2/P_2) + (x_3/P_3) \tag{10}$$

$$Q = \frac{(p_1-p_2)}{(\frac{x_1}{P_1}) + (\frac{x_2}{P_2}) + (\frac{x_3}{P_3})} \tag{11}$$

Case I

For Benzene:

Choose values from CBI report for polyurethane coated nylon fabric.
Test No. 17 - NYLON, Polyurethane coated

$Q = 0.0578$ lbm/ft$^2$ day

$A = 2.75$ ft$^2$

$x = 0.037$ in (= 0.0030833 ft)

Assume $p_2 = 0$

At 70$^o$ $p_1 = 79.4$ mm (= 0.10447 atm)

$$Q = \frac{P}{x}(p_1-p_2) \qquad P = \frac{Q\ x}{(p_1-p_2)} = \frac{(0.0578 \text{ lbm/(ft}^2\text{)day)(0.0030833 ft)}}{0.10447 \text{ atm}}$$

$$P = 0.0017058 \frac{\text{lbm}\quad \text{ft}}{\text{day ft}^2\quad \text{atm}}$$

For x = 0.037" (= 0.0030833 ft)

$$\frac{x}{P} = \frac{0.003083 \text{ ft}}{0.0017058 \frac{\text{lbm}\quad \text{ft}}{\text{day ft}^2\quad \text{atm}}} = 1.8073 \frac{\text{day ft}^2 \text{ atm}}{\text{lbm}}$$

$$\frac{x}{P} = 1.8073 \frac{\text{day ft}^2 \text{ atm}}{\text{lbm}}$$

Suppose Layer 2 is neoprene.

Use No. 6 stopper

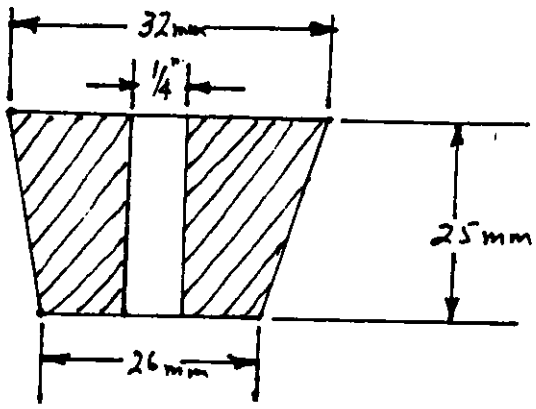


$$\text{Area for diffusion} = \frac{\pi[(32+26)/2]^2 \text{mm}^2}{4\ (25.4\ \text{mm/in})^2} - \frac{\pi(0.25)^2}{4}\ \text{in}^2$$

$A = (1.0238 - 0.0491) = 0.97471\ \text{in}^2$

$A = 0.006769\ \text{ft}^2$

$x = 25\ \text{mm} = 1\ \text{in}\ (= 0.08333\ \text{ft})$

From Diffusivity Calculation

$q = 0.0221\ \text{g/day}$

$$Q = \frac{0.0221\ \text{gm/day}}{0.006769\ \text{ft}^2 \times 453.59\ \text{gm/lbm}} = 0.0071978\ \text{lbm/(ft}^2\ \text{day)}$$

$$P = \frac{Q\ x}{(p_1 - p_2)} = \frac{0.0071978\ \text{lbm/(ft}^2\ \text{day)}\quad 0.08333\ \text{ft}}{0.10447\ \text{atm}}$$

$P = 0.0057249\ \text{lbm ft/(ft}^2\ \text{day atm)}$

$$\frac{x}{P} = \frac{0.08333\ \text{ft}}{0.0057249\ \text{lbm ft/(ft}^2\ \text{day atm)}}$$

$$\frac{x}{P} = 14.556\ \frac{\text{day ft}^2\ \text{atm}}{\text{lbm}}$$

From the composite seal

Let seal be as shown:

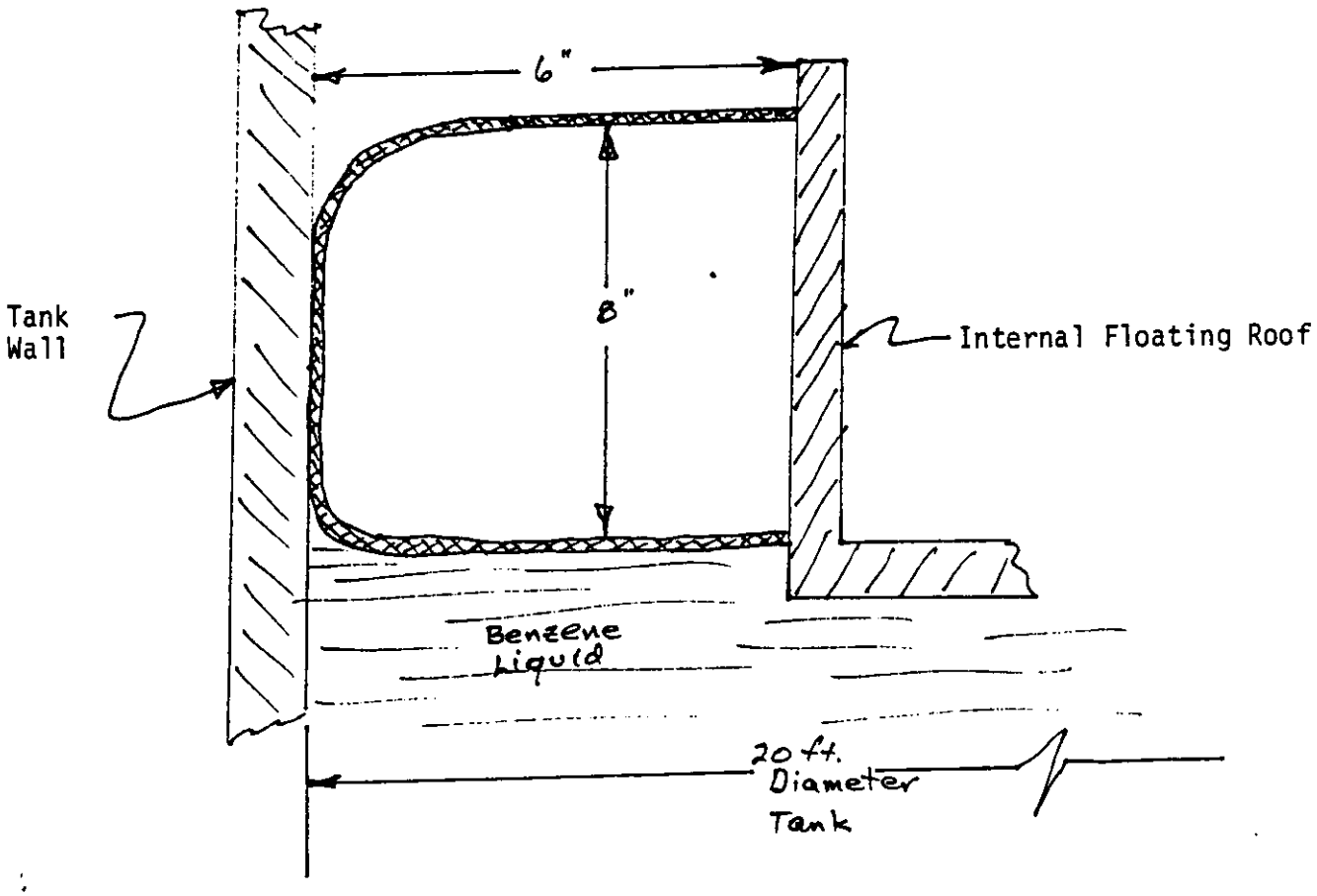

For Benzene at $70^{o}F$

$$Q = \frac{(p_1 - p_2)}{\frac{x_1}{P_1} + \frac{x_2}{P_2} + \frac{x_3}{P_3}}$$

$p_1$ = 79.4 mm (= 0.10447 atm)

$p_2 \doteq 0$

$x_1 = x_3$ - 0.037" thick

$$\frac{x_1}{P_1} = \frac{x_3}{P_3} = 1.8073 \frac{\text{day ft}^2 \text{ atm}}{\text{lbm}}$$

$x_2$ = 8" thick

$$P_2 = 0.0057249 \frac{\text{lbm ft}}{\text{ft}^2 \text{ atm day}}$$

$$Q = \frac{0.10447 \text{ atm}}{\left[2\ (1.8073) \frac{\text{day ft}^2 \text{ atm}}{\text{lbm}} + \frac{(8 \text{ in})}{(12 \text{ in/ft})\ 0.0057249 \frac{\text{lbm ft}}{\text{ft}^2 \text{ atm day}}}\right]}$$

$$Q = 8.695 \times 10^{-4} \frac{\text{lbm}}{\text{ft}^2 \text{ day}}$$

For 20' diameter tank:

Area for diffusion = $\frac{\pi}{4} [(20)^2 - (19)^2]$ ft$^2$

$$A = 30.6 \text{ ft}^2$$

For a year

$$q = 8.695 \times 10^{-4} \frac{\text{lbm}}{\text{ft}^2 \text{ day}} 30.6 \text{ ft}^2 \times 365 \text{ days/yr}$$

$$q = 9.7 \frac{\text{lbm}}{\text{yr}}$$

Case II - Petrex seal - $70^{o}F$

Will use neoprene permeability since we have no permeability for polyurethane foam.

Benzene Permeation:

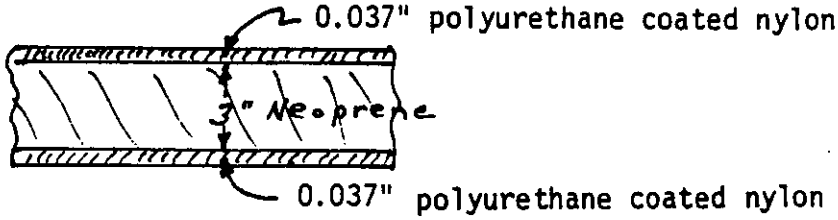


For polyurethane coated nylon:

$$\frac{x}{P} = 1.8073 \frac{\text{day ft}^2 \text{ atm}}{\text{lbm}}$$

For neoprene:

$$\frac{x}{P} = \frac{3 \text{ in}}{12 \frac{\text{in}}{\text{ft}} \; 0.0057249 \frac{\text{lbm ft}}{\text{ft}^2 \text{ atm day}}}$$

$$Q = \frac{(p_1 - p_2)}{\left[2\left(\frac{x_1}{p_1}\right) + \frac{x_2}{p_2}\right]}$$

$$= \frac{0.10447 \text{ atm}}{[2\ (1.8075) + 43.669]}$$

$$Q = 2.2094 \times 10^{-3} \frac{\text{lbm}}{\text{ft}^2 \text{ day}}$$

So for 20' diameter tank, 6" seal

$$q = 2.2094 \times 10^{-3} \frac{\text{lbm}}{\text{ft}^2 \text{ day}} \; 30.6 \text{ ft}^2 \times 365 \text{ days/year}$$

$$q = 24.7 \text{ lbm/year}$$

Case III Nitrile Rubber, 1" thick

Use data for glove no. 24 (the denser) of: Nelson, G.O., B.Y. Lum, G.J. Carlson, C.M. Wong, and J.S. Johnson, "Glove Permeation by Organic Solvents," American Industrial Hygiene Association Journal, 42, 217, March 1981

For Benzene

$Q = 510\ \mu g/min\ cm^2$

$x = 0.55$ mm

$$P = \frac{Q\ x}{(p_1-p_2)} = \frac{510\ \frac{\mu g}{min\ cm^2}\ 0.55\ mm}{(0.1251\ atm)}\ \frac{60\ \frac{min}{m} \times 24\ \frac{hr}{day}\ (2.54\ \frac{cm}{in})\ 144\ \frac{in^2}{ft^2}}{10^6\ \frac{mg}{g}\ 453.59\ \frac{g}{lbm}\ 25.4\ \frac{mm}{in}\ 12\ \frac{in}{ft}}$$

Tests were done at $25^oC$ (= $77^oF$)

For benzene

$$\log_{10}p = 6.97025 - \frac{1241.95}{t+223.781}$$

$p_i = 95.08$ mm (= 0.1251 atm)

$$P = 0.021696\ \frac{lbm\ ft}{ft^2\ day\ atm}$$

At $70^oF$

$x = 1"$ (= 0.08333 ft)

$$Q = \frac{P}{x}(p_1-p_2)$$

$$= 0.02696\ \frac{lbm\ ft}{ft^2\ day\ atm}\ \frac{0.10447\ atm}{(0.08333)\ ft}$$

$$= 0.02719\ \frac{lbm}{ft^2\ day}$$

For a year

$$q = 0.02719\ \frac{lbm}{ft^2\ day} \times 30.6\ ft^2 \times 365\ \frac{days}{year}$$

$$q = 304\ \frac{lbm}{year}$$

Case IV - 1" thick -- polyurethane coated nylon fabric

$$P = 0.0017058 \frac{\text{lbm} \quad \text{ft}}{\text{day ft}^2 \text{ atm}}$$

$$Q = \frac{P}{x}(p_1 - p_2)$$

For Benzene at 70°F

$$Q = \frac{0.0017058}{0.08333 \text{ ft}} \frac{\text{lbm}}{\text{day ft}^2} \quad \frac{\text{ft}}{\text{atm}} (0.10447 \text{ atm})$$

$$Q = 2.139 \times 10^{-3} \frac{\text{lbm}}{\text{day ft}^2}$$

$$q = 2.139 \times 10^{-3} \frac{\text{lbm}}{\text{day ft}^2} \times 365 \frac{\text{days}}{\text{year}} \times 30.6 \text{ ft}^2$$

$$q = 23.9 \text{ lbm/yr}$$

Case V - 2 layers of 0.037" thick nylon coated polyurethane

$$Q = \frac{0.10447}{2(1.8073)} = 0.0289 \frac{\text{lbm}}{\text{ft}^2 \text{ day}}$$

For a year

$$q = 0.0289 \times 30.6 \times 365$$

$$q = 323 \text{ lb/yr}$$

Case VI - Permeation through 2 layers of polyurethane covered nylon fabric plus 8" of stagnant air.

For a seal with two layers of polyurethane foam and air in between.

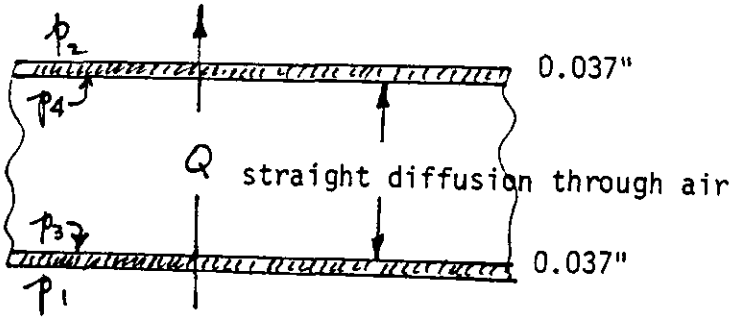

$$Q = \frac{P}{x}(p_1 - p_2)$$

$$Q = \frac{gm}{cm^2\ sec}$$

$$\frac{N_A}{A} = \frac{D_v \rho_m}{B_T} \ln \frac{1-y_A}{1-y_{Ai}}, \quad \frac{gm}{cm^2\ sec}$$

Through air

$$Q = \frac{D_v \rho_m}{B_T} \ln \frac{1-y_{A4}}{1-y_{A3}} \frac{}{(p_3 - p_4)} (p_3 - p_4)$$

$$= \frac{D_v \rho_m \ln \frac{1-y_A}{1-y_{Ai}}}{B_T\ (p_3 - p_4)} (p_3 - p_4)$$

$$R = \frac{B_T(p_3 - p_4)}{D_v \rho_m \ln \left(\frac{1-y_3}{1-y_4}\right)}$$

Need to estimate $p_3$ and $p_4$

$R_0 = R_1 + R_2 + R_3$

For the previous calculation using the resistances of the neoprene

$$\frac{x_1}{P_1} = 1.8073 \frac{day\ ft^2\ atm}{lbm}$$

$$\frac{x_2}{P_2} = \frac{8/12}{0.0057249} = 116.45$$

$$\frac{x_3}{P_3} = 1.8073$$

Total resistance = 120.0646

$$\frac{R_1}{(p_1-p_3)} = \frac{R_{overall}}{(p_1-p_2)}$$

$$\frac{1.8073}{(p_1-p_3)} = \frac{120.0646}{79.4 \text{ mm}}$$

$p_1 = 79.4$

$$(p_1-p_3) = \frac{1.8073}{(79.4)(120.0646)} = 1.195 \text{ mm}$$

$(p_1-p_3) = 1.195$ mm

$p_3 = 79.4-1.195 = 78.2$ mm; $y_3 = 78.2/760 = 0.1030$

$p_3 = 1.2$ mm ($p_3-p_4 = 0.1013$ atm) $y_4 = 1.2/760 = 0.00158$

For air

$$R = \frac{B_T \ (p_3-p_4)}{D_V \rho_m \ln \frac{1-y_4}{1-y_3}} \qquad D_V = 0.0879 \text{ cm}^2/\text{sec}$$

$$R = \frac{8/12 \text{ ft. } (0.1013 \text{ atm})}{0.0879 \text{ cm}^2/\text{sec} \ \ 4{,}076\text{x}10^{-5} \text{ gmole/cm}^3 \ \ 78{,}108 \text{ gm/gmole} \ \ \ln \left(\frac{1-0.00158}{1-0.1030}\right)}$$

$$R = 2.251 \frac{\text{ft atm sec cm}^3}{\text{cm}^2 \text{ gm}} \quad \frac{452.59 \text{ gm/lbm}}{2.54 \frac{\text{cm}}{\text{in}} \ \ 12 \frac{\text{in}}{\text{ft}} \ 60 \frac{\text{sec}}{\text{min}} \ \ 60 \frac{\text{min}}{\text{hr}} \ \ 24 \frac{\text{hr}}{\text{day}}}$$

$$R = 0.3880 \frac{\text{ft}^2 \text{ day atm}}{\text{lbm}}$$

Take an average:

$$\frac{120.0646 + 0.3880}{2} = 60.226$$

$$R = \frac{(8/12)(0.09817)(453.59)}{(0.0879)(4.076\times10^{-5})(78.108)(2.54)(12)(3600)(24)\ln((1-0.0031447)/(1-0.1013))}$$

$R = 0.3886$

Assume $R_2 = 1.8073$

Total R = 3 (1.8073)

$$\frac{1.8073}{p_1-p_3} = \frac{3\ (1.8073)}{79.4}$$

$$p_1-p_3 = \frac{79.4}{3} = 26.467$$

$p_3 = 79.4 - 26.467 = 52.933$ $\qquad y_3 = 0.0696487$

$p_4 = \qquad\qquad = 26.467$ $\qquad y_4 = 0.034825$

$(p_3-p_4) = 26.467$ mm $= 0.034825$ atm

$$R = 0.4103\ \frac{(0.034825)}{\ln\left(\frac{1-0.034825}{1-0.0696487}\right)}$$

$= 0.388859$

Let

$R_2 = 0.389$

$R_1 = 1.8073$

$R_3 = 1.8073$

$\Sigma R = 4.0036$

$$\frac{1.8073}{p_1-p_3} = \frac{4.0036}{79.4}$$

$p_3 = 79.4 - \frac{79.4\ (1.8073)}{(4.0036)} = 42.3079$ mm $\qquad y_3 = 0.0556683$

$p_4 = \qquad\qquad 37.09$ mm $\qquad y_4 = 0.0488026$

$p_3-p_4 = 5.2179$ mm

$(p_3-p_4) = 0.0068657$ atm

$$R = \frac{0.4108\ (0.0068657)}{\ln\left(\frac{1-0.0488026}{1-0.0556683}\right)}$$

$$= 0.388866$$

$$Q = \frac{0.10447}{4.0036} = 0.026094\ \frac{\text{lbm}}{\text{ft}^2\ \text{day}}$$

Q = 292 lbm/day  diffusion through 8" layer of air

Case VII - Two layers of 0.037" film + 1.0 in. of stagnant air

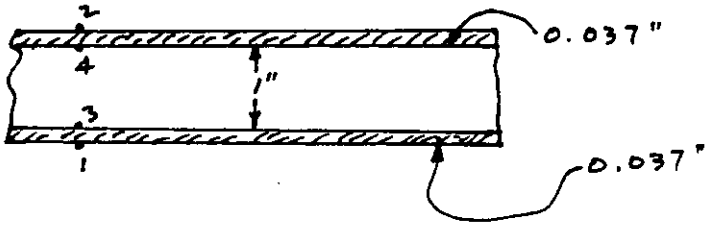


Let $R_1$, $R_3$ = 1.8073

Assume $R_2 = \frac{0.389}{8} = 0.04862$

$$\Sigma R = 3.663$$

$$\frac{1.8073}{p_1-p_2} = \frac{3.663}{79.4} \qquad p_1-p_3 = \frac{(79.4)(1.8073)}{3.663} = 39.175$$

$p_3$ = 79.4 - 39.175 = 40.224  $y_3$ = 0.05293

$p_4$ = 39.175  $y_4$ = 0.05155

$(p_3-p_4)$ = 1.049 mm (= 0.0013803 atm)

$$R_2 = \frac{0.05129\ (0.0013803)}{\ln\left(\frac{1-0.05155}{1-0.05293}\right)}$$

$R_2$ = 0.04862

$$Q = \frac{0.10447}{3.663} = 0.0285209$$

Q = 319 lb/yr

Case VIII


$R_{1"} + R_{8"} = 3.663 + 4.0036 = 7.666$

$Q = \frac{0.10477}{7.6666}$

$Q = 153$ lb/yr

Case IX

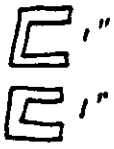


$R_{1"} + R_{1"} = 3.663 + 3.663 = 7.326$

$Q = \frac{0.10477}{7.326}$

$Q = 159$ lb/yr